Cosmic acceleration and the coincidence problem

Jean Claude Kubwimana

Department of Mathematics and Applied Mathematics

University of Cape Town

A thesis submitted in partial fullfilment of the degree of

Masters in Astrophysics and Space Science

August, 2009

I would like to dedicate this thesis to my loving parents, sisters and brothers.

Acknowledgements

First and foremost, I offer my sincere gratitude to my supervisor Prof. Bruce Bassett for his support, valuable advice and encouragement throughout this work. An instructive climate of sharing ideas and discussions on different subjects in cosmology that he always encourages in our group is of great importance especially for young researchers; I can't forget that.

My work was also enriched by members in our cosmology group: Dr. Marco Regis, Dr. Matthew Smith, Dr. Petja Salmi, Renee Hlozek, Yababel Tadesse, Melvin Varughese; their comments helped me to learn more about how to write in a more concise and consiting way. I will always keep in mind the time everyone spent on reading my thesis draft.

I am also indebted by the help from Dr. David Bacon and the hospitality offered by the Institute of Cosmology and Gravitation (ICG) in Portsmooth, England for a period of about six months to carry out my research. Dr. David Bacon and Mr. Cristiano Sabiu from the ICG accepted to read my very drafty thesis version. I owe them a lot for that.

I finally thank the NRF (National Research Fund) through the NASSP (National Astrophysics and Space Science Programme) for funding this dissertation component for my Masters degree, and the Royal Society-NRF bilateral exchange for finding my visit to the ICG.

Abstract

In the standard model of the Universe, the cosmos has only accelerated once since decoupling and only recently, at around a redshift of $z \simeq 0.5$ as supported by different observations including Type Ia Supernovae (SNIa), the Cosmic Microwave Background (CMB), Large Scale Structure (LSS), and Weak Lensing (WL). This confirmation however, lacks a fundamental physics explanation. The hypothetical form of energy termed 'dark energy' (DE) assumed to account for that acceleration behavior, is still mysterious and why its dominance only occurred recently is a profound problem widely known as the coincidence problem. So far all attempts for resolving the coincidence the problem have been unsatisfactory. Here we investigate a possible solution to the coincidence problem in the form of multiples phases of acceleration (MPA). If there were more than one phase of acceleration between now and decoupling, then the current phase of acceleration would be much less special, alleviating the coincidence problem. We use a modified Markov Chain Monte Carlo (MCMC) technique together with the WMAP five year TT data to search for parameters allowing a second phase of acceleration. Despite extensive search we find no models that simultaneously fit the WMAP data and yield a second phase of acceleration, ruling out this particular set of models as the solution to the coincidence problem.

Contents

List of Figures

Chapter 1

Introduction

Over the last decade, the Universe has been observed to have an accelerating expansion that started at redshift $z \sim 0.5$, in contrast to previous beliefs suggesting that it has been slowing down. This discovery was confirmed on the basis of Supernovae Ia (SN Ia) observations (Riess *et al.* (1998), Perlmutter *et al.* (1999a)) and afterwards, observations from the Cosmic Microwave Background (CMB) (Spergel *et al.* (2003)), Large Scale Structure (LSS) (Abazajian *et al.* (2004)) and Weak Lensing (WL) (Linder (2004)). Although this accomplishment is among the most exciting in modern cosmology it has also ignited lots of issues and challenges to cosmology as well as related fields.

In order to account for the accelerating behavior of the Universe the standard cosmology favors a cosmological constant (CC) Λ. It was initially introduced by Einstein as a new component of the stress-energy tensor in his general relativity field equations, in order to account for a repulsive gravity and thus make the Universe static. The idea was abandoned later after the discovery of the expansion of the Universe by Hubble in 1926, which is well known as 'Einstein's greatest blunder'. The cosmological constant came back again in 70's (Gunn & Tinsley (1976); Sulentic *et al.* (2007)), introduced to explain some observations, like quasars distribution at high redshift, Hubble diagrams of clusters, and the age of the Universe problem. The standard cosmology, is usually referred to as ΛCDM, because it also relies on a theory of structure formation based on clustering induced by cold dark matter (CDM). Nowadays ΛCDM with initial

conditions provided by the inflation theory fits remarkably well the current cosmological data.

In classical general relativity, the CC has the dimension of $[length]^{-2}$ and it is just a constant of nature that one has to determine experimentally. On the other hand quantum fluctuations in the vacuum act as contribution to the CC, which can be computed from quantum field theory. The vacuum energy in Quantum Chromodynamics (QCD), Electroweak, Grand Unified Theory (GUT), Planck energy scales can be estimated as $\sim 10^{36}, \sim 10^{47}, \sim 10^{102}, \sim 10^{110}\ erg/cm^3$ respectively (Carroll (2001); Shapiro (2008)). However the vacuum energy associated to the CC was found to be $\rho_{\Lambda}^{ex} \sim (10^{-10})\ erg/cm^3$; thus, there is a need for some unknown contributions to cancel the quantum fluctuations contribution and fine tune Λ by 46-120 orders of magnitude. This is a fundamental issue for the physical meaning of the CC, known as the CC problem.

Another related issue to the accelerating nature of the Universe is that the vacuum density normally doesn't change with time but other components of the Universe like radiation and matter density do as the Universe expands. The reason why it is only at low redshift that the Universe become vacuum energy dominated is of high priority to know because if it had happened at any earlier epoch the Universe would have evolved differently. Based on current theory, the ratio of the matter and vacuum decreases as a^{-3}, with a, the Universe scale factor, which evolves with time. Clearly it is only within a limited period in which observers can witness simultaneously the vacuum energy density to matter density ration to be $\sim O(1)$ and the transition from matter dominated epoch to vacuum dominated epoch. There is yet no convincing physical reason why this transition is happening at the present time; thus it is referred to as the coincidence problem.

Different models were built around the scalar field theory attempting to explain the acceleration of the Universe, without the cosmological constant (or, at least with a negligible energy compared to the global dynamics of the Universe). Some models assume a hypothetical form of energy termed "Dark Energy"(DE), with a constant equation of state $w = p\rho^{-1} \neq -1$ (the ratio of pressure to density), or an equation of state evolving with redshift z, $w(z) = p\rho(z)^{-1}$. Those include:

- Quiessence. This model uses $w = constant$, and $w = -1$ is a special case corresponding to the cosmological constant Λ (Lazkoz (2007)).

- Quintessence models treat dark energy as a slowly varying scalar field with a potential V obeying different conditions to try tracking dark energy behavior (Caldwell *et al.* (1998), Kolda & Lyth (1999)).

- "Phantom" DE models allow even very negative equation of state $w = p/\rho < -1$ (but can lead to unclear physical interpretation and develop instabilities at the quantum level) (Caldwell *et al.* (2003), Wang *et al.* (2004)).

- Modified gravity DE where gravity is modified at cosmological scales to try to explain the late time cosmic acceleration. The representative of the generalized modified theories of gravity are the $f(R)$ theories which involve adding to the Ricci scalar R in the Einstein action an arbitrary curvature function $F(R)$ to allow it to be renormalizable (Sotiriou & Faraoni (2008)).

- Chaplyin gas model using $p\rho \propto -1$, as the equation of state and $\rho = (A + B(1+z)^6)^{1/2}$ (Chakraborty & Debnath (2007); Debnath (2007)).

We will describe more on some of these models in Chapter (2). Other models include Oscillating DE, Interacting DE, Scalar-Tensor DE, Holographic DE, etc. For details on the mentioned models see Sahni & Starobinsky (2006) and references therein.

Other alternatives were built around parametric and non-parametric reconstruction of quantities and functions directly related to dark energy. The luminosity distance, the DE density, DE equation of state w_{de}, etc. In the parametric case the most common way is expanding the quantity into Taylor series up to a certain number of terms. Alternatively, instead of a Taylor expansion, one can describe the dark energy equation of state through a different ansatz (Bassett *et al.* (2002)), or using the principle components method (Huterer & Starkman (2003)). The non-parametric reconstruction involves the use of some smoothing of quantities binned appropriately in the redshift space (Wang & Lovelace (2001)), and also kinematic description which uses quantities directly related to the expansion of the Universe (e.g the scale factor a, the Hubble parameter H, or the deceleration parameter q) and modification of general relativity theory to explain the cause of cosmic acceleration.

The goal of this thesis is to propose a new class of solutions to the cosmic coincidence problem by suggesting a particular dynamical nature of dark energy through some special parameterization accounting for a second phase of acceleration after decoupling. With such a class of solution we may be able to check:

- Whether the current acceleration of the Universe is unique since decoupling: there have been another phase of acceleration in the more distant past and maybe others will happen in future.
- Dark energy exhibits dynamical behavior and therefore $w \neq constant$.
- Do the parameters used to obtain a second phase of acceleration allow a good fit to current CMB data?

In the next chapter we give a brief review on the Universe most favored description (isotropic and homogeneous) focusing on the cosmic acceleration and coincidence problem. In Chapter three we describe our parameterization and toy test of our model. In Chapter four we give a more robust test of our model via Monte Carlo sampling method and finally in Chapter five we discuss our results and draw conclusions.

Chapter 2

The Universe and acceleration

This chapter covers basic concepts and some of current approaches used in measuring different quantities in modern cosmology. We concentrate on descriptions and ideas behind its mysterious current acceleration and the coincidence problem. In the following section we cover basic concepts in cosmology, in section (2.2) we explain how structures in the Universe formed and their impact on its current accelerating expansion. In section (2.4), we describe the CMB anisotropy. In section (2.5), we give more details on cosmic acceleration and its evidences.

2.1 Brief introduction to cosmology

The cosmological principal says that no point in the Universe is preferred, which allows the assumptions that in a set of spatial surfaces in a spacetime, all physical properties of the Universe don't change with direction (isotropic) and are the same at all points (homogeneous). These two assumptions are were also found to be in agreement with large scale ($\gg 10Mpc$) (Spergel *et al.* (2003)), distribution of galaxies, and the quasi-uniformity of CMB. The spacetime metric describing such a universe has the familiar Friedmann Robertson walker (FRW) line element

$$ds^2 = dt^2 - a^2(t)\left(d\chi^2 + f_K(\chi)^2 d\Omega^2\right). \tag{2.1}$$

where $d\Omega^2 = d\theta^2 + sin^2\theta d\phi^2$, χ is the comoving radial distance (a massive particle at rest in comoving coordinates remains at rest, and a freely moving one will come to rest in those coordinates. See section (2.2) for more details about its dynamics),

and θ, ϕ are angular coordinates, t corresponds to time, a the scale factor. $f_K(\chi)$ corresponds to the 3-dimensional space curvature with

$$f_K(\chi) = \begin{cases} \frac{1}{\sqrt{K}} \sin(\sqrt{K}\chi) & \text{if } (K > 0) \\ \chi & \text{if } (K = 0) \\ \frac{1}{\sqrt{-K}} \sinh \sqrt{-K}\chi & \text{if } (K < 0) \end{cases} \tag{2.2}$$

where K is the space curvature. Note we used coordinates where c=1, and unless mentioned, will adopt the same value for the remainder of this work. Equation (2.1) which was originally introduced due its mathematical simplicity was later found to be a good representation of the Universe on large scales, see for example the discussion in Silvestri & Trodden (2009).

2.1.1 Cosmological redshift

The scale factor characterizes the size of the Universe, and the momentum of a freely moving particle scales as $1/a(t)$ what introduces the stretching of wavelength or redshift of photons from a distant galaxy. The Hubble's law (Hubble (1929)) relates the recession velocity v of an object to its comoving distance χ via $v = H\chi$, with $H = \dot{a}/a$, the Hubble parameter, we can write

$$dv = \frac{\dot{a}}{a} d\chi. \tag{2.3}$$

The Doppler shift relation gives the change in frequency of the emitted waves due to the motion of the emitter. We then can write

$$\frac{d\lambda}{\lambda_e} = \frac{dv}{v} = \frac{da}{a}, \tag{2.4}$$

where the second equality is due to relation (2.3). Integrating both sides of (2.4) yields

$$\frac{\lambda_r}{\lambda_e} = \frac{a(t_r)}{a(t_e)} = 1 + z, \tag{2.5}$$

where e and r indexes refer to quantity at emission and reception respectively, and $\lambda_r/\lambda_e = 1 + z$, with z the cosmological redshift. This relation tells us about the size of the Universe via the scale factor $a(t_e)$. In addition, the time intervals are related to the redshift through

$$dt = -\frac{dz}{H(z)(1+z)}. \tag{2.6}$$

Equation (2.6) can help to determine the age of the Universe as we will see later.

2.1.2 Friedmann Equations

When the FRW metric is considered in solving the Einstein field equations

$$G_{\mu\nu} = 8\pi G T_{\mu\nu} - g_{\mu\nu}\Lambda, \tag{2.7}$$

where $G_{\mu\nu} = R_{\mu\nu} - (1/2)Rg_{\mu\nu}$, $g_{\mu\nu}$ is the metric tensor, Λ is the cosmological constant, $R_{\mu\nu}$, the Ricci tensor, R the Ricci scalar and $T_{\mu\nu}$ the energy-momentum tensor, one can obtain

$$\left(\frac{\dot{a}}{a}\right)^2 = \frac{8\pi G\rho}{3} - \frac{K}{a^2} + \frac{\Lambda}{3}, \tag{2.8}$$

and

$$\frac{\ddot{a}}{a} = -\frac{4\pi G}{3}(\rho + 3p) + \frac{\Lambda}{3}, \tag{2.9}$$

which are Friedmann equations and the acceleration equation respectively. In these equations ρ is the energy density, p the pressure which includes all the Universe's contents, and $\Lambda = 8\pi G\rho_{vac}$; with ρ_{vac} the vacuum density.
From the equations (2.8) and (2.9) one can easily get the continuity equation

$$\dot{\rho} = -3H(\rho + p), \tag{2.10}$$

and to make a complete set of equations to describe both the geometry and the evolution of the Universe, one has also to consider the equation of state relating the energy density and pressure

$$w = p/\rho. \tag{2.11}$$

For simplicity w is considered to be constant although it is expected to change with redshift. Using the equation of state and the continuity equation yields an important relation,

$$\rho \propto a^{-3(1+w)}. \tag{2.12}$$

For relativistic (radiation) and non-relativistic particles(dark matter,baryons) we have $w_r = 1/3$ and $w_{m0} = 0$ respectively leading respectively to $\rho_r = \rho_{r0}(1+z)^4$ and $\rho_m = \rho_{m0}(1+z)^3$. Therefore radiation dilutes faster than matter. In the case of a universe with $N(i = 1, ...N)$ different fluids the above equation can be put into the form

$$\rho = \sum_{i=1}^{N} \rho_{i0} a^{-3(1+w_i)}, \tag{2.13}$$

and the Friedmann equation becomes

$$\left(\frac{\dot{a}}{a}\right)^2 = \frac{8\pi G}{3}\sum_{i=1}^{N}\rho_{i0}a^{-3(1+w_i)} - \frac{K}{a^2} + \frac{\Lambda}{3}. \tag{2.14}$$

For the present epoch and considering a flat universe (K=0) the above equation yields

$$\sum_{i=1}^{N}\Omega_{i0} + \Omega_\Lambda = 1, \tag{2.15}$$

where we have defined the density parameter of the i-th component as

$$\Omega_{i0} \equiv \frac{\rho_{i0}}{\rho_c} = \frac{8\pi G}{3H^2}\rho_{i0} \tag{2.16}$$

with $\rho_c = 3H_0^2/8\pi G$ the critical density, which is the density required to make the current Universe flat, and $G = 1.88 \times 10^{-29}h^2 gcm^{-3}$ the gravitational constant and

$$\Omega_\Lambda = \frac{\Lambda}{3H^2}. \tag{2.17}$$

We also define

$$\Omega_K = \frac{K}{a^2H^2}, \tag{2.18}$$

which is the Universe curvature density parameter. There is also a relation between the density parameter Ω and the spatial curvature of the Universe: For $\Omega_0 > 1$, the Universe's spatial curvature is positively curved; for $\Omega_0 < 1$, the Universe's spatial curvature is negatively curved; for $\Omega_0 = 1$, the Universe's spatial curvature is flat. This shows that a FRW universe is mainly characterized by the Hubble constant H_0 and four density parameters: Ω_m, Ω_r, Ω_K and Ω_Λ. Another important quantity to mention here is the deceleration parameter, $q(z)$ defined as

$$q(z) = -\frac{\ddot{a}}{aH^2} = \frac{1}{2}\sum_i \Omega_i(z)[1 + 3w_i(z)], \tag{2.19}$$

that can tell us by how much the Universe acceleration has increased.

Realistic measurements have been done by Millimiter wave Anisotropy eXperiment IMaging Array (MAXIMA), Balloon Observations Of Millimetric Extragalactic Radiation ANd Geophysics (BOOMERANG), Cosmic Background Explorer (COBE) (Jaffe *et al.* (2001)), and most recently, Wilkinson Microwave Anisotropy Probe (WMAP) (Komatsu *et al.* (2009)) in order to gain accurate

values of different cosmological parameters. Assuming ΛCDM model, the current Universe was found to be spatially flat, with only $\sim 5\%$ of visible content (baryonic matter) and a large dark side of $\sim 95\%$ made of $\sim 72\%$ of dark energy believed be responsible for acceleration of the Universe and of $\sim 23\%$ of dark matter (NASA (2008b)) introduced mainly to explain why galaxy rotation curves are flat .

In Figure (2.1) it is shown how the contents of the Universe contents evolved and that the current Universe is vacuum (or dark energy) dominated.

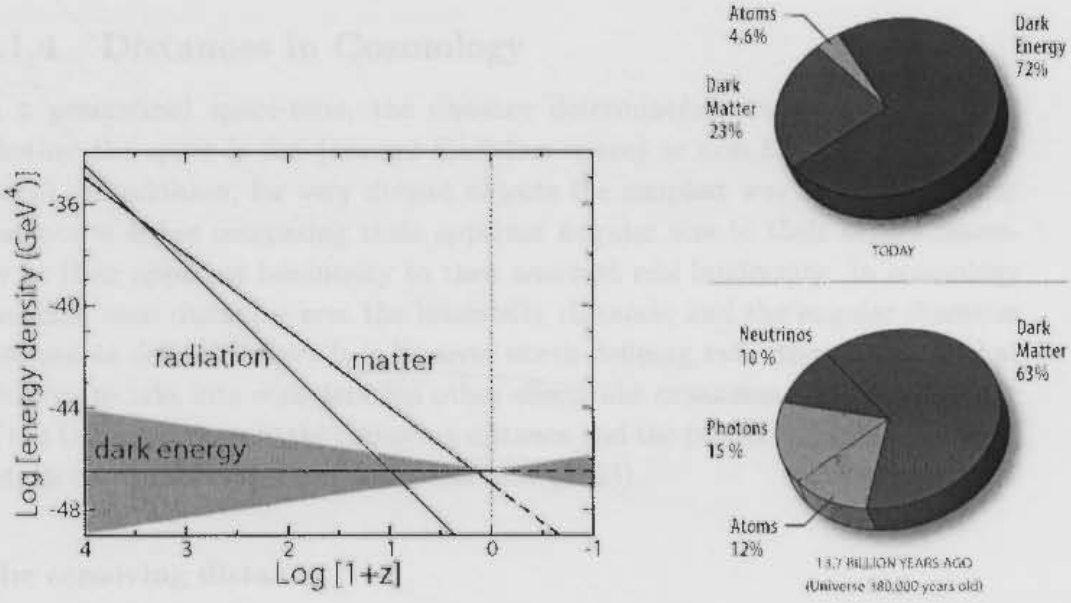

Figure 2.1: *Universe content in the early and late universe, the band represent* $w = -1 \pm 0.2$ (Frieman *et al.* (2008), NASA/WMAP/Science/Team (2009)).

2.1.3 Age and principal epochs of the Universe

From equations (2.6) and (2.13) and neglecting Ω_{r0} because at late time it is small compared to other components

$$t_0 = \frac{1}{H_0} \int_0^1 da[a^{-1}\Omega_m + (1 - \Omega_m - \Omega_\Lambda) + a^2\Omega_\Lambda]^{-1/2}. \qquad (2.20)$$

The easiest case to solve is when the Universe is matter dominated and hence $\Omega_m \simeq 1$ and, $\Omega_\Lambda = 0$ which gives $t_0 = 2/3H_0$.

The radiation energy scales as $\rho_r \propto a^{-4}$ as shown in equation (2.12). In the early Universe ($t \to 0$) radiation dominates over other components and from Friedmann equation (2.14) we get $a(t) \propto \sqrt{t}$. At late time however ($t \to \infty$) radiation is negligible; and using the same equation and assuming a flat universe we find that $a(t) \propto t^{2/3}$. In both cases we have assumed that the cosmological constant is zero.

2.1.4 Distances in Cosmology

In a generalized space-time, the distance determination requires us to know whether the space is flat (normal Euclidian space) or non flat (open or closed space). In addition, for very distant objects the simplest way to measure their distance is either comparing their apparent angular size to their actual diameter or their apparent luminosity to their assumed real luminosity. In cosmology the most used distances are: the luminosity distance, and the angular diameter distance as defined below. It is however worth defining two other distances that allow us to take into consideration other effects like expansion and the geometry of the Universe, namely the comoving distance and the proper distance. For more details on distances one can check Harrison (1993)

The comoving distance

This is the distance between the source world-line and an observer world-line comoving with the expansion of universe. Coordinatewise, if an observer is at z_1 and the source at z_2, for photons $ds = 0$, we then can find from the metric that

$$d_c(z_1, z_2) = \chi(z_1, z_2) = \frac{c}{H_0} \int_{a(z_2)}^{a(z_1)} [a\Omega_m + a^2(1 - \Omega_m - \Omega_\Lambda) + (a)^4\Omega_\Lambda]^{1/2} da, \quad (2.21)$$

the comoving distance simplifies calculations a lot especially in complicated metric elements. It is then assumed in almost all analysis involving the Universe geometry. Most authors assume the comoving distance to be non dynamic i.e not changing between two given comoving observers. Any particle moving with respect to the comoving coordinates has a so called peculiar velocity which decays as $1/a$ unless it is supported by inhomogeneous matter distribution.

The proper distance

This is refers to the distance which is measured using the travel time of a ray of light reaching an observer at z_1 at time t_2 from a source at z_2 at time t_2. It is then defined as $d_p = -c\int dt = -c\int (aH)^{-1} da$ which leads to

$$d_p(z_1, z_2) = \frac{c}{H_0}\int_{a(z2)}^{a(z_1)} [a^{-1}\Omega_m + (1 - \Omega_m - \Omega_\Lambda) + (a)^2\Omega_\Lambda]^{1/2} da. \tag{2.22}$$

The proper distance in contrast to comoving distance is assumed to be changing between two observers and then at low redshift (or within small range of redshift) coincides with the comoving distance.

Angular diameter distance

If we consider an observer at redshift z_1 and object at redshift z_2 with the physical cross section δA and solid angle $\delta\omega$ the angular diameter distance is given by

$$d_A(z_1, z_2) = \sqrt{\frac{\delta A}{\delta\omega}}. \tag{2.23}$$

The solid angle $\delta\omega$ is related to the cross section δA via

$$\frac{\delta\omega}{4\pi} = \frac{\delta A}{4\pi a^2(z_2) f_K^2[\chi(z_1, z_2)]}, \tag{2.24}$$

using the above relation into (2.23) we can write

$$d_A(z_1, z_2) = a(z_2) f_K[\chi(z_1, z_2)]. \tag{2.25}$$

This distance is important for the estimation of how far away is an astronomical object is. The relation (2.25) is valid in any FRW universe.

The luminosity distance

Objects for which we know luminosity are called 'standard candles', naturally there are rare. The most used ones so far are type Ia supernovae. They are very bright and can be found out to cosmological distances.The luminosity distance is defined as

$$d_L = \left(\frac{L}{4\pi F}\right)^{\frac{1}{2}}, \tag{2.26}$$

where F is the observed flux from the standard candle, L its intrinsic luminosity. In relation to the emitted luminosity L_e the flux is given by

$$\frac{L_e}{4\pi a(t_r)^2 f_K^2(\chi)(1+z)^2}, \tag{2.27}$$

leading to

$$d_L = (1+z)a(t_r)f_K(\chi). \tag{2.28}$$

In relation to the angular diameter distance, the luminosity distance is also given by

$$d_L(z_1, z_2) = (1+z)^2 d_A(z_1, z_2). \tag{2.29}$$

The above relation is valid in any space-time and shows that photons are redshifted by $(1+z)$, the angular diameter distance and the flux are then reduced by a factor of $(1+z)^2$ and $(1+z)^4$ respectively. Figure (2.2) compares the four mentioned distances. All the distances almost coincide at low redshift.

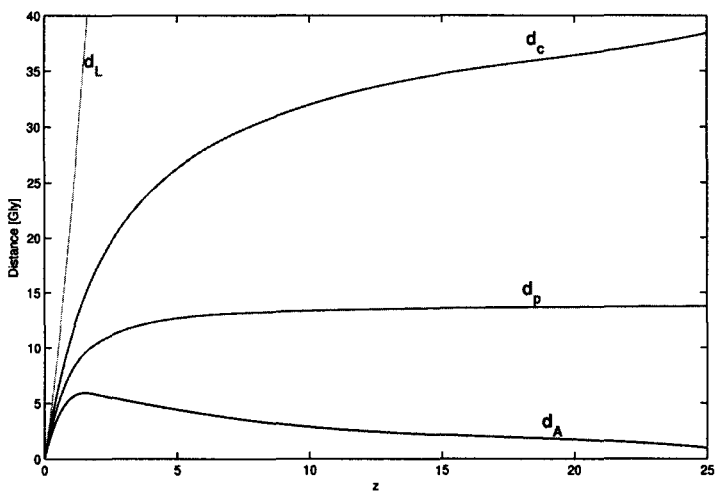

Figure 2.2: *Comparison of the four distances measures d_A, d_p, d_c, and d_L in a flat universe with $\Omega_m = 0.3$, $\Omega_\Lambda = 0.7$ and $H_0 = 70.0 kms^{-1}M_{pc}^{-1}$.*

2.1.5 Hubble diagram

Standard candles are supposed to have fixed absolute magnitude M which is the apparent magnitude an object would have if viewed at 10 parsecs away from the

observer. If we substract the measured logarithmic energy flux m, we obtain distance modulus $\mu = m - M$ which is used to constrain cosmological models using the luminosity distance d_L via and using equations (2.27) and (2.28)

$$\mu(z) = 5\log_{10}\left(\frac{d_L}{10pc}\right) \tag{2.30}$$

This relation is also known as the magnitude-redshift relation. This is visualized with the Hubble diagram (Figure (2.3)). If one Taylor expands the scale factor $a(t) = 1 + H_0(t - t_0) - (q_0 H_0)^2(t - t_0)/2 + ...$, then

$$H_0 d_L = z + \frac{1}{2}(1 - q_o)z^2 + ... \tag{2.31}$$

This is a test for acceleration or deceleration of the Universe if one considers the deviation from the linear case which is the usual Hubble law.

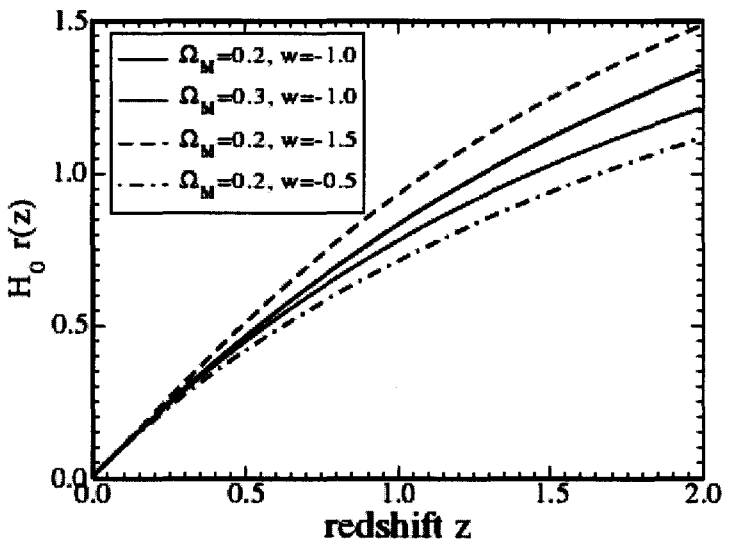

Figure 2.3: *The effect that dark energy has on cosmic distance shown through different values of* Ω_m *and* w *in a flat universe* (Frieman *et al.* (2008)).

2.2 Structure formation

There is a reasonably precise prediction and explanation of the observed large structures in the Universe by simply performing the linear perturbation of involved quantities (Marcos *et al.* (2006), Bernardeau *et al.* (2002)). The simplest case is the Newtonian limit valid for scale $r \ll cH^{-1}$ and non relativistic case $v/c \ll 1$. The ideal fluid equations, namely conservation equation, Euler equation(relativistic) and Poisson equation in the comoving coordinates $\vec{x} = \vec{r}/a$ with a peculiar velocity $\vec{v} = a\dot{\vec{x}}$, can be put respectively into

$$\dot{\rho}(\vec{x},t) = -\frac{1}{a}\vec{\nabla}\cdot[(1+\delta(\vec{x},t))\vec{v}] \tag{2.32}$$

$$\dot{\vec{v}} + \frac{1}{a}(\vec{v}\cdot\vec{\nabla}_r)\vec{v} + \frac{\dot{a}}{a}\vec{v} = -\frac{1}{a}\vec{\nabla}_r\phi$$

$$\nabla^2\phi = 4\pi G\delta\bar{\rho}a^2\delta \tag{2.33}$$

where we have introduced the dimensionless density contrast $\delta(\vec{x},t) = (\rho(t) - \bar{\rho})/\bar{\rho}$, with $\bar{\rho}$ corresponding to the background density and we have neglected the pressure term in the Euler equation as $\vec{\nabla}p/\rho \ll \vec{\nabla}\phi$. Only taking into account the linear perturbation regime one may write the first two equations above as

$$\dot{\delta} + \frac{1}{a}\vec{\nabla}\vec{v} = 0 \tag{2.34}$$

$$\dot{\vec{v}} + \frac{\dot{a}}{a}\vec{v} + \frac{1}{a}\vec{\nabla}\phi \tag{2.35}$$

Taking the time derivative of the first equation, dividing the second by the scale factor a, subtracting one from the other, and making use of both the continuity and the Poisson equations yields

$$\ddot{\delta} + 2H\dot{\delta} + \left(\frac{c_s^2k^2}{a^2} - 4\pi G\bar{\rho}\right)\delta_k = 0, \tag{2.36}$$

with $c_s = \partial p/\partial\rho$ the sound speed and k the wavenumber. It is also important to define here the Jean's wavenumber $k_J^2 \equiv 4\pi G\bar{\rho}a^2/c_s^2$ which characterizes gravitationally stable and unstable modes. For short wave modes $k \gg k_J$ perturbations oscillate as a sound wave $\delta(t) \sim exp(\pm i\omega t)$ with $\omega = c_sk/a(t)(1-n)$ and we have assumed that $a(t) \propto t^n$. For long wavelength modes with $k \ll k_J$, the above equation is expected to have a growing mode (D_+) and a decaying mode

(D_-). We then can write its solution as $\delta(\vec{x},t) = A(\vec{x})D_+(t) + B(\vec{x})D_-(t)$ and the perturbation equation takes the form

$$\ddot{D} + 2H(z)\dot{D} - \frac{3}{2}\Omega_{m0}H_0^2(1+z)^3 D = 0, \tag{2.37}$$

which is known as the linear growth factor equation.

The simplest solution is obtained for a dust dominated universe with $\Omega_m = 1$, for which $D_+(t) \propto t^{2/3} \propto a(t)$ and $D_-(t) \propto t^{-1} \propto a^{-3/2}$. We are here interested only in the growing case as it is the one falling in the scenario of structure formation. In general, $d\ln D_+/d\ln a \simeq \Omega_m$; this implies that as Ω_m goes below one, the growth slows down. For $\Omega_m \neq 1$, $D_+(t)$ is rather complicated. The case for $\Omega_m \neq 0$ is treated in (Peebles (1980)).

The growth of structure analysis explains why the early universe (at time t $\ll$ 300000 yrs) was very homogeneous and how it ended up having structures (stars, galaxies, clusters,...) with different overdensities: stars ($\delta\rho/\rho \sim 10^{30}$), galaxies ($\delta\rho/\rho \sim 10^5$), clusters of galaxies ($\delta\rho/\rho \sim 10 - 10^3$), superclusters ($\delta\rho/\rho \sim 1$), and so on. In a flat universe, the growth of the linear density perturbations ceases when dark energy begins to dominate (Frieman *et al.* (2008)). The redshift corresponding to that is estimated through $z = (\Omega_{de}/\Omega_m)^{-1/3w_{de}} - 1$. The other effect is imposed by the equation of state where higher values of the equation of state makes dark energy to become dominant earlier, and thus stops the growth earlier. Therefore for the growth factor to have a small value since decoupling it is necessary for the perturbations to keep a large amplitude between the redshift for reionizationz_{re} and the current redshift z_0 (Frieman *et al.* (2008)). We also would expected it to be nearly uniform for scale $l \ll cH^{-1}$.

2.3 Power spectrum and Transfer function

In a flat universe, we can work in Fourier space and define the components of δ to be

$$\delta(\vec{x},t) = 2\pi \int d^3k \delta_k e^{2\pi i \vec{k}\cdot\vec{x}}, \tag{2.38}$$

with

$$\delta_k = 2\pi \int d^3x \delta(\vec{x}) e^{-2\pi i \vec{k}\cdot\vec{x}}, \tag{2.39}$$

In the case of a Gaussian field different phases in the field $\delta(\vec{x})$ are uncorrelated and the probability distribution of δ is also Gaussian,

$$p(\delta) = \frac{1}{\sqrt{2\pi\sigma^2}} \exp(-\delta^2/2\sigma^2), \tag{2.40}$$

where σ^2 is the variance and is given by

$$\sigma^2 = 4\pi \int_0^\infty 2P(k)dk, \tag{2.41}$$

where the quantity $P(k)$ is the power spectrum given by $P(k) = \langle A_k A_k^* \rangle$ and $A_k = \delta_k \exp(-i\theta_k)$ and $A_k^* = \delta_k \exp(i\theta_k)$. The power spectrum gives the information about the density fluctuation as a function of scale. Its shape is preserved at linear scales and grows proportional to $D^2(t)$.
An other quantity to define in the linear theory power spectrum is the transfer function $T(k)$

$$P(k,t) \propto kT^2(k)D_+^2(t), \tag{2.42}$$

$T(k)$ describes the fluctuations growth after they reenter into the horizon. $T^2(k)$ is constant at large scales but equal to $T^4(k)$ at small scale (Eisenstein & Hu (1997)).

2.4 The cosmic microwave background

This subsection discusses mainly the cosmic microwave background radiation and its impact on acceleration by putting some constrains on parameters involved in detecting dark energy which is the potential candidate for causing the Universe expansion to accelerate. We will describe the CMB power spectrum, and how its measurements are affected by different contaminations.

The cosmic microwave background is a fair picture of the radiation fluid at the time of decoupling at redshift $z \simeq 1100$. In its early history, the Universe was opaque due to the inverse compton scattering in the photon-baryon plasma. Later on, its expansion temperature decreased to around $T \simeq O(1)eV$, corresponding to decoupling redshift, electrons and nucleons recombined, the Universe started to become transparent and photons can propagate freely. At the beginning those photons were highly energetic but as the Universe expands they get cooler and cooler and now they can be detected only in microwave band. As the scale factor

scales as $a \propto 1/T$, with T the temperature of the Universe, and considering that radiation was dominating in the early universe with $\rho_r \propto T^4$, one can even compute the age of the Universe at any temperature through $\left(\dot{T}/T\right)^2 \propto 8\pi G T^4/3$ (Hu & Dodelson (2002)).

2.4.1 Anisotropies in the CMB radiation

The cosmic microwave radiation measured by the Cosmic Background Explorer (COBE) and Wilkson Microwave Anisotropy Probe (WMAP) satellites showed some temperature fluctuations of order of 10^{-5} (Smoot *et al.* (1992)). Those fluctuations have been mainly sourced from following physical effects: the peculiar velocity of the last scattering surface, radiation field intrinsic fluctuations on the last scattering surface, fluctuations in the gravitation potential on the last scatterring surface also known as the Sachs Wolfe effect, which is a dominant fluctuation source mainly on large scales, $\Theta \gg 1^0$, with Θ the angle substended on the last scattering surface (Gaztanaga *et al.* (2006), Afshordi *et al.* (2004)). We give more description about this effect below.

Fluctuations on large scales are mainly primordial ones and on small scales we observe those which entered the horizon before decoupling, and therefore show the photon-baryon acoustic oscillations. Those were damped by gravity and radiation pressure. It is then expected to have the maximum amplitude of oscillations on fluctuations that entered the horizon just before decoupling i.e $D \sim H_{ls}^{-1}$ or the horizon size.

The Sachs Wolfe (SW) effect and the Integrated Sachs Wolfe effect(ISW)

Gravitational fields can alter the energies of photons and therefore can make their wavelength longer(redshifted) of shorter(blueshifted). This happens to some of the photons from the last scattering surface as they cross the potential wells caused by matter overdensity. This is called the Sachs Wolfe effect named after Rainer Kurt Sachs and Arthur Michael Wolfe (Sachs & Wolfe (1967); Sapone *et al.* (2009)). For the CMB this appears as an effect on temperature change $\delta T/T$. The ordinary Sachs Wolfe effect would just correspond to the depth of each potential well in which the photon was at the time of the last scattering. This won't affect the CMB fluctuations as any shift in the photons wavelength

would equally affect all the CMB.

On the other hand if we consider all the paths of the photon to us, with the photon falling in and climbing different potential wells, the key thing would be to check if the depth potential well Ψ changes while the photon is crossing since the shift is proportional to Ψ. The ISW is then estimated through the formula (Gaztanaga *et al.* (2006))

$$\Delta^{ISW}(\vec{n}) \approx -2 \int dz \frac{d\Psi[\chi(z), \vec{n}, z]}{dz}, \tag{2.43}$$

where $\vec{n}$ is the photons direction along the line of sight.

$$\frac{d\Psi}{dz} \propto \frac{d[(1+z)\frac{\delta_k(z)}{\delta_k(0)}]}{dz} \equiv \frac{dD}{dz}, \tag{2.44}$$

In the radiation dominated era we have an early IS effect, and in matter dark energy dominated Universe($z < 1$) a late ISW effect. We can consider linear perturbations at very large scales; photons from the CMB would have gone though a large number of potential wells which will slightly affect the CMB power spectrum at large angles. Cross correlations between CMB map and LSS map are used to measure this effect. Its effect should be correlated with the matter distribution in the local universe if potentials are decaying at late time (Boughn & Crittenden (2004); Fosalba & Gaztanaga (2004)). The resulting signal indicates that $\Omega_m \neq 1$, good evidence that our Universe is not described by the de Sitter model.

Satellite experiments (COBE, WMAP), balloon experiments (MAXIMA, BOOMERANG), and ground based experiments were done in order to measure the fluctuations in the CMB temperature. In addition the recently launched Planck satellite is expected to give unprecedented precision in the measurements of those fluctuations. The ISW effect was shown in the WMAP observations and can also be seen as cold spots in the produced CMB map (Scranton *et al.* (2003))

The peaks in the CMB power spectrum in Figure (2.4) corresponds to oscillations in the photon-baryon plasma which entered the horizon before decoupling and were propagating at the speed of sound. The highest points the size at the decoupling which is expected to be same as the horizon size. Those oscillations usually termed Baryon Acoustic Oscillations (BAO) are also imprinted in matter power

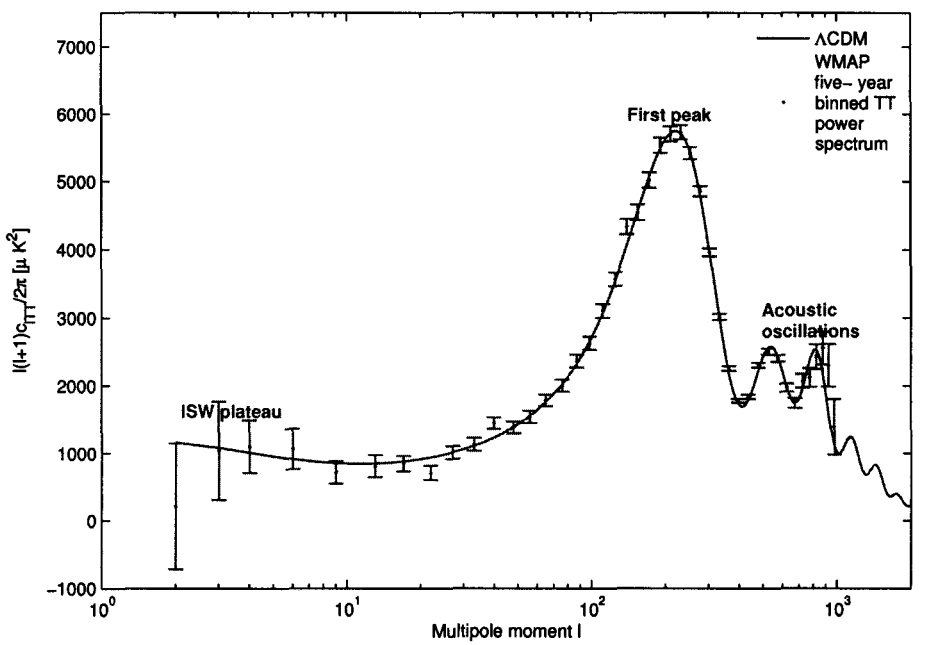

Figure 2.4: *CMB power spectrum obtained using CAMB (Lewis* et al. *(2000)). Lower l are affected by the ISW and at large l, we have acoustic peaks. The ΛCDM model was considered (solid line) for fitting data points.*

spectrum and provide a new way of measuring distances at different redshift and therefore called standard ruler.

The ISW is expected to have a strong correlation with the matter around us, and is powerful probe of dark energy therefore providing an important way to distinguish between different acceleration models. It was also found that the ISW puts constraints on the equation of state parameter w and dark energy density Ω_{de}. Figure(2.5) shows those constraints at 68% and 95% confidence levels.

It is often preferred to expand the CMB temperature anisotropy into spherical

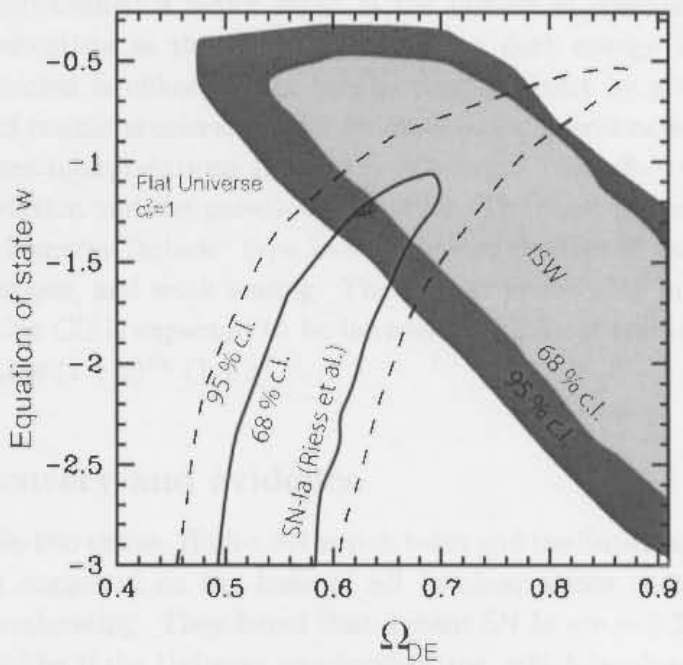

Figure 2.5: *Constraints on w and Ω_{de} using ISW and Supernovae surveys* (Corasaniti *et al.* (2005)).

harmonics

$$\frac{\delta T}{T}(x_0, t_0, \vec{d}) = \sum_{l,m} a_{l,m}(x_0) Y_{l,m}(\vec{d}), \tag{2.45}$$

where x_0 is our position, t_0 is the time at present, $\vec{d}$ is the direction of observation, and l's are the different multipoles. We also have that

$$\langle a_{l,m} a^*_{l',m'} \rangle = \delta_{l,l'} \delta_{m,m'} C_l, \tag{2.46}$$

where $\delta_{l,l'}$ and $\delta_{m,m'}$ factors represent Kronecker delta functions, and C_l are called CMB power spectrum.

2.5 Cosmic acceleration and the coincidence problem

As we said in our introduction, the discovery of the accelerating expansion of the Universe represented a major event in the history of cosmology but a big challenge for scientists as the exact nature of the dark energy that might be causing acceleration is unknown. In this section, we start by giving details of the discovery of cosmic acceleration and its observational evidences, and then we describe different interpretations given to dark energy. This effect in turn affects the distance relation and the growth of structure. The most promising methods in probing dark energy include: type Ia supernovae, clusters of galaxies, baryon acoustic oscillations, and weak lensing. The highest probability in detecting deviations from the CC is expected to be between redshifts of few tenths and two because $\rho_{de}/\rho_m \propto (1+z)^{3w}\ (1+z)^{-3}$.

2.5.1 Discovery and evidence

In the late 1990s two teams, High-z SN search team and the Supernova Cosmology Project (SCP) suggested on the basis of SN Ia observations that the Universe expansion is accelerating. They found that distant SN Ia are ~ 0.25mag dimmer than they would be if the Universe was decelerating, which implies that, for past 5 Gyrs, the Universe was accelerating instead of the opposite behavior that was commonly believed at that time (Perlmutter *et al.* (1999a); Riess *et al.* (1998), Frieman (2008)). Since then, many other sources supported those observations including the Supernova Legacy Survey (SNLS) and ESSENCE (Goldhaber *et al.* (2001), Astier *et al.* (2006), Miknaitis *et al.* (2007)). This was an important breakthrough in cosmology regardless of ambiguities it created and the lack of concrete theoretical explanations. Other independent sources that were used to confirm the accelerating expansion of the Universe include CMB, LSS, BAO, and WL observations. We describe briefly those sources and observations below. For more details, one may also read (Amsler *et al.* (2008); Frieman *et al.* (2008); Frieman (2008)) and references therein.

Type Ia Supernovae

White dwarfs, mainly in the process of mass accretion to a companion star can cross the Chandrasekhar limit ($\sim$ 1.4 solar masses) and the result is a violent explosion called a type Ia supernova. Supernovae are very bright, and can be observed from high redshift($z \sim 1$). Their main spectroscopical characteristics is a singly-ionized silicon line at 615nm near maximum brightness. The common explosion mechanism leads to a high expectation that, SNe Ia have uniform intrinsic luminosity but in reality there is a scatter of about 15% (Frieman *et al.* (2008)). High redshift supernovae measurements require particular care due to systematic errors. Going to space or observing in the near infrared bands would minimize photometric errors.

Supernovae Ia were confirmed to be standard candles in the 1990s. A universe with just matter and a cosmological constant responsible for acceleration was inferred with a confidence level of 99% (Perlmutter *et al.* (1999b)). See Figure (2.6) for details. More supernova observations confirmed those results up to recent analysis. But later some authors raised the problem that extinction due to dust is the factor causing SN Ia to appear fainter rather than the cosmic acceleration (Simonsen & Hannestad (1999)). However, recently high quality light curves were generated from the high redshift Hubble Space Telescope observations have reinforced initial discovery that the Universe acceleration is the cause of the observed effect in supernovae rather than dust (Riess *et al.* (2000)).

Already in the 1990's an empirical correlation was established between SN Ia peak and decay rate after the peak. It was found that brighter SN Ia decay slower than fainter ones. Distances to high and low redshift SNe Ia are used to constrain cosmological parameters. This is done via the distance modulus formula modified to be $m - \Pi = 5log_{10}[H_0 d_L(z; \Omega_m, \Omega_{de}, w(z))]$ with $\Pi = M - 5log_{10}(H_0 M_{pc}) + 25$ the effective parameter constrained by low redshift SNe in the Hubble diagram (see Figure (2.6)).

For realistic measurements one has to correct for different contaminations namely the host galaxy extinction and uncertainty about the intrinsic colors of supernovae Ia. Those errors can lead to distance uncertainties even for observations in more than one band (Frieman *et al.* (2008)).

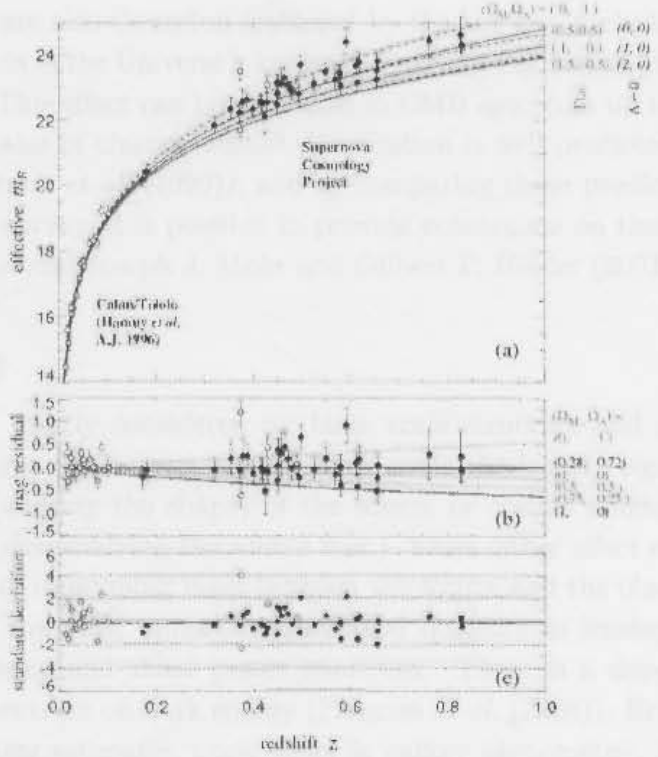

Figure 2.6: *Using different Ω_m, Ω_Λ sets: the top panel is the Hubble diagram from the Supernova Cosmology Project (Carroll (2001)),the middle panel corresponds to the magnitude residual, and the bottom panel shows the number of standard deviations of each point from the best-fit curve.*

CMB and Large scale structure

Primordial fluctuations are expected to have grown and lead to the structures we observe today. Dark energy has a huge impact on growth and can only dominate recently in order to allow structure to form as it is. The distance to the last scattering surface, estimated to be ($z \simeq 1100$) via CMB measurements, would be also affected if there is no content with a large negative pressure. For CMB to help in probing dark energy, it has to be associated with other measurements, mainly because it is just one snapshot of when dark energy was subdominant; it is however a standard ruler for BAO measurements.

CMB photons are also Compton scattered by the hot gas in clusters (the largest virialized objects in the Universe), known as Sunyaev-Zel'dovich (SZ) effect (Burigana (2007)). This effect can be measured in CMB spectrum up to high redshift. Dark matter halos of cluster redshift distribution is well predicted from N-body simulations (Frenk *et al.* (1999)); and by comparing those predictions to an extended cluster survey, it is possible to provide constraints on the cosmic history (Zoltan Haiman and Joseph J. Mohr and Gilbert P. Holder (2001)).

Weak lensing

Another effect mostly considered for large scale structure and galaxies, is the deflection of light due to gravity. On large scale the lensing signal can lead to cosmic shear (altering the shape) of the source or cosmic magnification effects (amplifying or deamplifying the source flux). From either effect one can directly infer the mass of intervining mass between the source and the observer along the line of sight. The most important statistical quantity in lensing measurement is the convergence and shear power spectrum. There is a dependency of the shear power spectrum on dark energy (Frieman *et al.* (2008)). Errors introduced by incorrect shear estimates, uncertainty in galaxy photometric, intrinsic galaxy shape correlations, point spread function can be a hindrance in detecting the lensing signal, but with forthcoming powerful telescopes like DES (Dark Energy Survey) (DES-project (2009)), LSST (Large Snaptic Survey Telescope) (Ivezic *et al.* (2008)), DUNE (Dark Universe Explorer) (Refregier *et al.* (2006)), etc. a lot will be achieved in this area.

Baryon acoustic oscillations

Wiggles in the CMB spectrum are the signature of the BAO. These signatures also appear in the matter power spectrum although their amplitude are lowered by non linear growth. SDSS Luminous red galaxies provide a high detection of those oscillations, and their scales corresponds to the sound horizon scale at recombination. As the BAO amplitude power sectrum is determined by how those fluctuations grow since the recombination epoch z_{re} and the BAO redshift z_{BAO}, it is also possible to measure the growth factor by comparing the CMB power spectrum at recombination and the galaxy power spectrum, and this in turn can be used to constrain the history of the Universe within z_{re} and z_{BAO} range.

2.5.2 Coincidence problem

As discussed in the previous sections, the matter density scales with the Universe expansion as $\rho_m \sim 1/a^3$, and the vacuum energy density $\rho_\Lambda \simeq$constant, which implies that there is only one epoch in the Universe history when $\rho_m \sim \rho_\Lambda$. The reason why that epoch happens to be ours is hard to explain. One has to find out whether that coincidence is an important clue in understanding cosmic acceleration or just a result of different scalings of energy densities in the Universe and its age.

Roughly the time for dark energy dominance happens when its energy density $\rho_{de} \propto a^3\rho_m$ or $\Omega_{de} \propto a^3\Omega_m$. the corresponding ratio $r = \Omega_{de}/\Omega_r$ tends to zero in the past and grow in the future. We will describe in next subsection some of approaches base on dynamical dark energy which tried to solve the coincidence problem as well as the cause of cosmic acceleration.

2.5.3 Dark energy models

Dark energy models are either dynamical or non-dynamical depending on whether its behavior is allowed to change with time or to be invariant. In more details there are

- Models with the cosmological constant (i.e $w = -1$).
- Models with the constant w (i.e. $w \neq -1$, also called Quiessence) (domain walls:$w = -2/3$, cosmic string: $w = -1/3$,...) (Lazkoz (2007)).
- Models with dynamical w (Quintessence, Chaplygin gas, K-essence, braneworld) (Caldwell *et al.* (1998), Kolda & Lyth (1999)).
- Models with $w < -1$ (Phantom models, braneworld cosmology) (Caldwell *et al.* (2003), Wang *et al.* (2004), Chimento *et al.* (2009)).
- Modified gravity DE models which put the usual gravitational Lagrangian in terms of the scalar curvature R into a Lagrangian depending on arbitrary function F(R) (Sotiriou & Faraoni (2008)).

Other models include: Holographic dark energy, Scalar-tensor models, etc. For a more complete list and description see Cahn *et al.* (2008); Sahni & Starobinsky (2000). We describe some of those models below:

Constant Dark energy

In the case of constant dark energy or vacuum energy with a certain parameter value Λ termed cosmological constant, the constant Λ is inserted in Einstein field equation

$$R_{\mu\nu} - \frac{1}{2}g_{\mu\nu}R = 8\pi G T_{\mu\nu} - \Lambda g_{\mu\nu}. \tag{2.47}$$

Λ then acts as an isotropic and homogeneous source and lead to the negative pressure $p_{de} = -\rho_{de}$, and . The standard cosmological model (ΛCDM) assumes the Friedmann metric, zero curvature and a non-dynamical dark energy; so far however, all the attempts to compute the value of Λ lead to the CC problem as we even said in the introduction. Calculations of the vacuum expectation value of the energy momentum for both bosonic and fermionic fields lead to a divergent integral due to the wave number k^4 (Frieman *et al.* (2008))

$$< T_{00} >_{vac} \propto \int_0^\infty \sqrt{k^2 + m^2 k^2} d^3k \simeq \frac{k_{max}^4}{16\pi^2}. \tag{2.48}$$

By imposing the quantum level limit to be at the Planck scale, $< T_{00} >_{vac} \simeq c^5/G\hbar \sim 10^{110} erg/cm^3$ which is much larger than the current measured value ($\rho \simeq 10^{-10} erg/cm^3$) by 120 orders of magnitude. Rescaling down to QCD scale also helps to lower the order to 46 orders of magnitude. Other attempts introduce the supersymetric (SUSY) particles where bosonic and fermions in standard model of particle physics have their SUSY counterparts and due to their opposite signs and the matching degree of freedom, they can cancel and lead to zero contribution at least up to some scale M_{susy} where SUSY is not broken. This also however only reduces by 15 orders of magnitude (Frieman *et al.* (2008); Sahni & Starobinsky (2000)).

Quintessence

A different approach resides in concentrating on mass-energy sources in the Universe (Caldwell *et al.* (1998)). This is possible by assuming the scalar field ϕ, with a potential $V(\phi)$ and a Lagrangian

$$L = \frac{1}{2}g^{\mu\nu}\partial_\mu\phi\partial_\nu\phi - V(\phi), \tag{2.49}$$

The corresponding energy momentum tensor has the form $T_{\mu\nu} = \partial_\mu\phi\partial_\nu\phi - g_{\mu\nu}[g^{\gamma\delta}\partial_\gamma\phi\partial_\delta\phi + V(\phi)]$. If one assumes a perfect fluid, the equation of state takes the form

$$w_\phi = \frac{p_\phi}{\rho_\phi} = \frac{\dot{\phi}^2/2 - V(\phi)}{\dot{\phi}^2/2 + V(\phi)}, \tag{2.50}$$

where ϕ is the scalar field, ρ_ϕ and p_ϕ are energy density and pressure corresponding to ϕ. The equation of motion is the Klein -Gordon equation which has the form

$$\ddot{\phi} + 3H\dot{\phi} + \partial V/\partial\phi = 0. \tag{2.51}$$

In order for acceleration to happen the equation of state has to be negative. In addition it is needed that the energy associated to the potential $V(\phi)$ only starts acceleration recently and be at least of the same order as the currently measured Ω_{de} value. Different $V(\phi)$ have been suggested so far, and two most popular are: the inverse power law potentials $V(\phi) = M^4(\phi/M_p)^{-n}$ and exponential potentials $V(\phi) = M^4\exp(-\alpha(\phi/M_p))$, where M is the mass scale, and α is adimensionless parameter (Kolda & Lyth (1999)). For the latter case, in the FRW regime, also using equation (2.51) it is possible to show that acceleration can be achieved for $\alpha^2 < 2$ (Sahni & Starobinsky (2000)). There also exist solutions by tracking DE behavior that can help in solving the Coincidence problem. However, It is still hard to provide a reason why the generated potentials should remain stable. Quintessence models are also confronted with a fine-tuning problem when it comes to the mass scale which is usually too small (Copeland *et al.* (2006)).

K-Essence

By modifying the kinetic term in the Lagrangian one can get a different approach known as K-essence (Armendariz-Picon *et al.* (2000)).

$$L(\phi, X) = K(X) - V(\phi), \tag{2.52}$$

where $X = \frac{1}{2}g^{\mu\nu}\partial_\mu\phi\partial_\nu\phi$. In the case of homogeneous form for ϕ, $X = -\frac{1}{2}\dot{\phi}^2$, the equation of state takes the form

$$w_\phi = \frac{p}{\rho} = \frac{K(X) - V(\phi)}{[2X(\partial K/\partial X)(X)] + V(\phi)}. \tag{2.53}$$

One should also ensure that $\rho > 0$ and that the speed of sound $c_s^2 = (\partial p/\partial\rho) > 0$ for a stable theory. It was found that the scalar field ϕ can naturally evolve, and for a wide range of initial conditions, it is possible to track the DE density in matter and therefore give an important clue of why it started dominating only recently (Copeland *et al.* (2006)).

Phantom dark energy

Conventionally in general relativity, in order to avoid vacuum instabilities and the propagation of energy outside the light cone, the possible energy momentum tensors are defined through the following energy conditions: i) The weak energy condition ($\rho \geqslant 0$ and $\rho + p \not\geqslant 0$.); ii) The null energy condition ($\rho + p \geqslant 0$); iii) The dominant energy condition ($\rho \geqslant p$); iv) The null dominant energy condition (Negative energies are allowed if $\rho = -p$); v) The strong energy condition $\rho + p \geqslant 0$ and $\rho + 3p \geqslant 0$.); Many authors based on what the data may allow, suggested the violation of the null dominant energy condition and studied the so called 'phantom' component case with ($w < -1$) (Hoyle & Narlikar (1964), Caldwell (2002), Corasaniti *et al.* (2004)). Although it is easy to construct a model where there is no future singularity, it is also possible to get rid of the big rip by choosing a suitable scalar field in a such a way that $w < -1$ can settle back to $w \geq -1$, those models were found to lead to quantum instability (Nesseris & Perivolaropoulos (2004)).
In Figure (2.7) we also show constraints upon the equation of state $w(z)$ and the Ω_m done by (Caldwell & Doran (2004)) constrained in the case of quintessence models via different measurements (CMB and SNe).

2.5.4 Reconstructing Dark energy

Clearly there is a large number of models trying to explain the behavior of dark energy a potential candidate for acceleration. By looking at the quantities directly related to dark energy namely $w(z)$, $d_L(z)$ or $H(z)$ it is possible to think about a model independent way of reconstructing the properties of DE by just fitting observations. Using $w(z)$ has the advantage that it is closely related to the underlying physics because, it is given by $p\rho^{-1}$ but can be less powerful if cosmic acceleration would be caused by new gravitational physics (Frieman *et al.* (2008)). Other techniques for creating fitting functions include (as we also mentioned in the introduction): Direct reconstruction, Principle component analysis, and a Kinematic description. We will however describe here the $w(z)$ parameterization, for other cases ($d_L(z)$ or $H(z)$) and methods see Frieman *et al.* (2008); Sahni & Starobinsky (2000) and references therein.

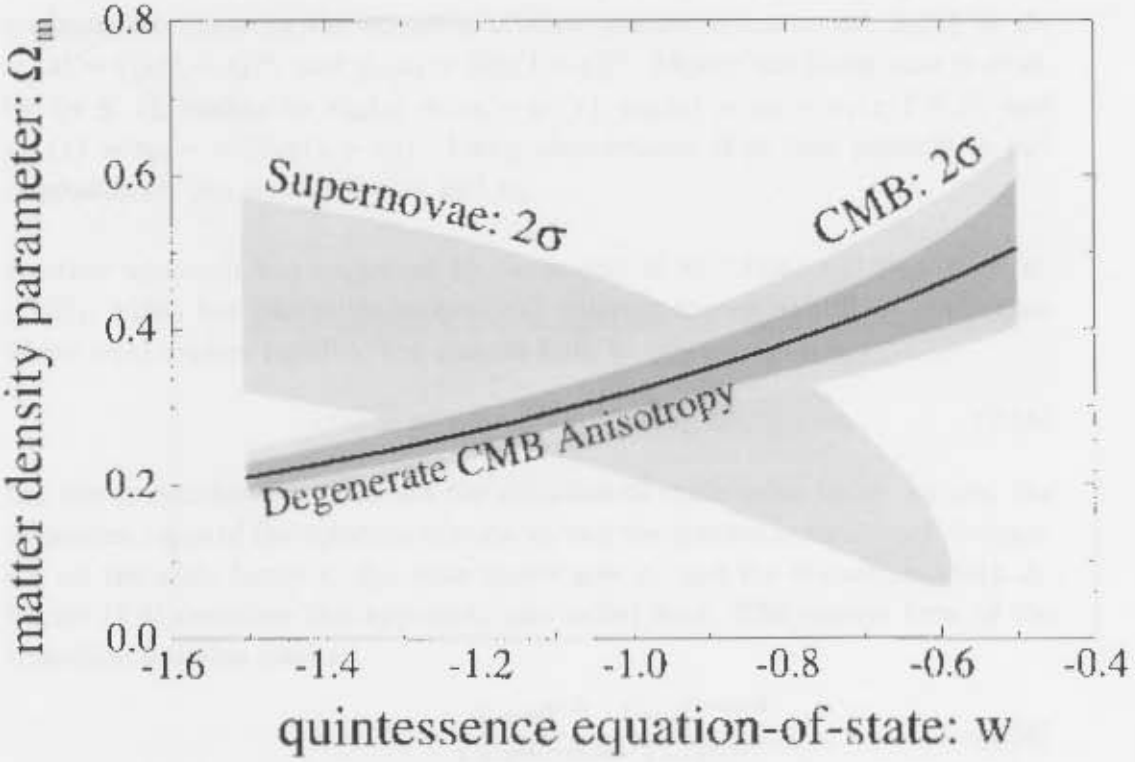

Figure 2.7: Constraints on Ω_m and w using WMAP, ACBAR, CBI data surveys (Caldwell & Doran (2004)).

Equation of state parameterization

A number of parameterizations have been suggested so far, where most of them use Taylor series expansion of $w(z)$ using a particular functions $x_n(z)$(n=0,...,N).

$$w(z) = \sum_{n=0} w_n x_n(z). \tag{2.54}$$

The simplest case is for constant w where $x_0(z) = 1$ and $x_n = 0$ $(n \geq 1)$. Other common functions for the equation of state parameterization are $x_n(z) = z^n$, $x_n(z) = ((z/1+z))^n$, and $x_n(z) = [log(1+z)]^n$. Mostly the linear case is studied $(n \leq 1)$, leading to $w_{de}(z) = w_0 + w_1(z)$, $w_{de}(z) = w_0 + w_1(z/1+z)$, and $w_{de}(z) = w_0 + w_1([log(1+z)])$. Using observations, it is then possible to put constaints on two parameters w_0 and w_1.

Another approach was suggested by Corasaniti *et al.* (2004) and Bassett *et al.* (2002), which has particular property of allowing tracker solutions in the case where $w(z)$ evolves rapidly. The general form in this approach is

$$w(a) = w_0 + (w_1 - w_0)\Gamma(a, a_t, \Delta), \tag{2.55}$$

the five parameters involved are the equation of state value today w_0 and the maximum value of the equation of state w_1 and the transition function Γ depending on the scale factor a, the scale factor now a_1 and the transition width Δ. Figure (2.8) describes this approach, also called *kink*. The general form of the transition function used is

$$\Gamma(a, a_t, \Delta) = \frac{1 + e^{a_t/\Delta}}{1 + e^{(a_t - a)/\Delta}} \frac{1 - e^{(1-a)/\Delta}}{1 - e^{1/\Delta}}. \tag{2.56}$$

For redshifts $z < z_1$, $w(z)$ is nearly a constant and abruptly changes to higher values within a transition of width Δ, to a maximum value $w = w_m = w_1$. The redshift at which the acceleration stage starts z_c was found to be strongly dependent on the $w(z)$ parameterization (Bassett *et al.* (2004)), z_c value consistent with the estimation is $w = -1$ (ΛCDM case) with $z_c = 0.66^{+0.11}_{-0.11}$, other cases like $w(z) = w_0 + w_1 z$ and $w(z) = w0 + w_1 z(1+z)^{-1}$ give $z_c = 0.14^{+0.14}_{-0.05}$ and $z_c = 0.59^{+8.91}_{-0.21}$ respectively (Copeland *et al.* (2006)).

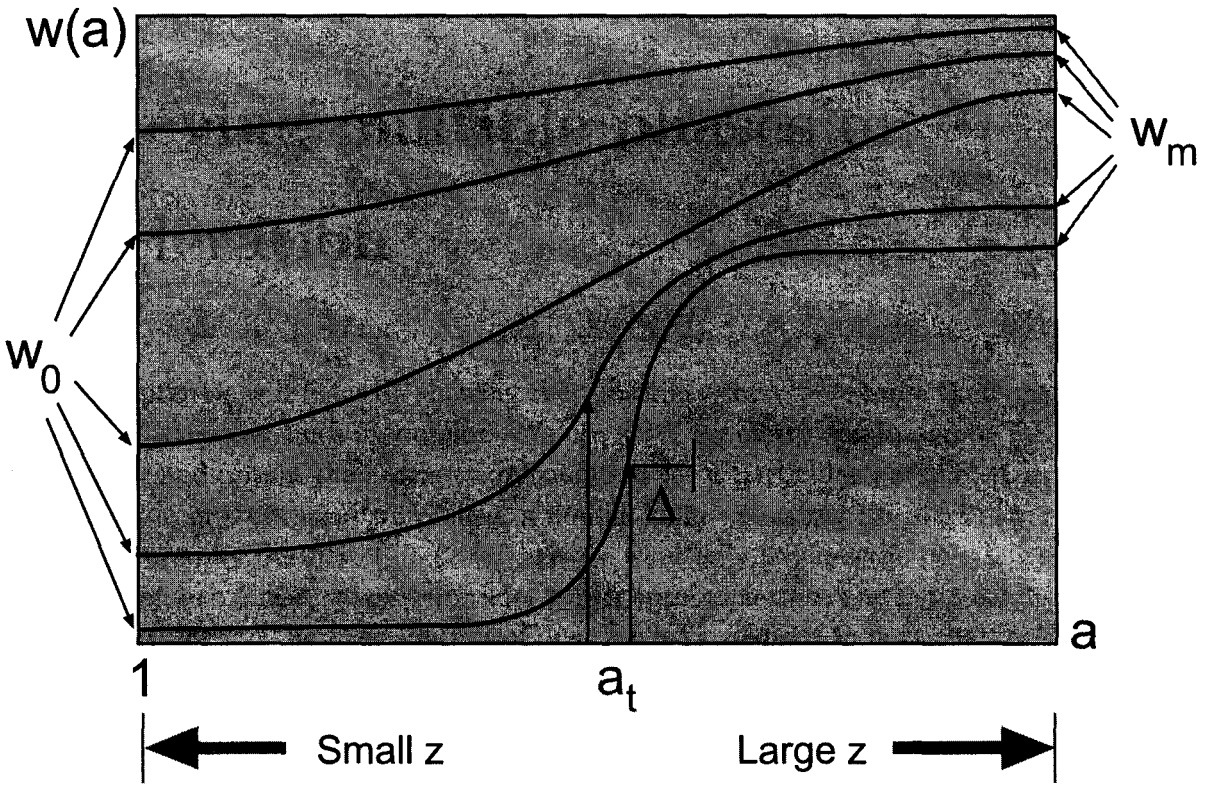

Figure 2.8: *Illustration of a typical kink approach for the equation of state parameterization* (Corasaniti *et al.* (2004)).

Chapter 3

Achieving multiple phases of Acceleration

In this chapter we will focus on showing the possibility there were more than one phase of acceleration since decoupling. We use FRW geometry dominated by DE and matter and obtain the acceleration condition for a particular parameterization equation of state $w(z)$ which uses a double kink, extending the single kink first introduced by Bassett *et al.* (2002). As we want only to show the possibility of more than one phase, we only consider rough approximations and get a condition for acceleration. Further analysis of our case is carried out in next chapters. The Friedmann equations with no cosmological constant take the form

$$\left(\frac{\dot{a}}{a}\right)^2 = \frac{8\pi G}{3}\rho - \frac{K}{a^2}, \tag{3.1}$$

$$\frac{\ddot{a}}{a} = -\frac{4\pi G}{3}(\rho + 3p), \tag{3.2}$$

where the overdot denotes a derivative with respect to time, a is the scale factor related to the redshift z via $a = (1+z)^{-1}$, K is the curvature parameter, ρ and p refer to the total the energy density and the total pressure of all current dominant components of the Universe (matter,dark energy) respectively. Throughout the remainder of this work we will adopt this notation.

Generally the parameter w_i is not constant and evolves with time. From the continuity equation for each component $\dot{\rho}_i/\rho_i = -3(1+z)^{-1}(1+w_i)$ one can

relate its evolution to the redshift and the energy density as

$$f(z) = \frac{\rho_i}{\rho_{i0}} = \exp\left[3\int_0^z d\ln(1+z')(1+w_i(z'))\right], \tag{3.3}$$

where the index 0 denotes the value today. Particularly constant w_i leads to

$$\rho_i = \rho_{i0}(1+z)^{3(1+w_i)}. \tag{3.4}$$

Considering a flat Universe ($K = 0$) having two components: dark energy characterized by w_{de} and non-relativistic matter with $w_m = 0$ we can write the acceleration equation as

$$\frac{\ddot{a}}{a} = -\frac{4\pi G}{3}\left[\rho_m + \rho_{de}(1+3w_{de})\right]. \tag{3.5}$$

From equations (3.5) and by including the density parameter $\Omega_i = 8\pi G\rho_i/3H^2$ one can also write the acceleration in terms of redshift as

$$\frac{\ddot{a}}{a} \propto -\Omega_m(1+z)^3 + (1-\Omega_m)(1+3w_{de}(z))f(z). \tag{3.6}$$

Obviously from the acceleration equation we get for the Universe with only one component the necessary condition to accelerate ($\ddot{a} > 0$). For our two component universe case however we will need

$$(1-\Omega_m)(1+3w_{de}(z))f(z) > \Omega_m(1+z)^3, \tag{3.7}$$

which was derived from equation (3.6). In the case of constant $w_i(z)$ the condition is $w_i \leq -1/3$, which is mostly used in fudicial models (quiessence) of dark energy and it is straight forward to derive, but in the case of evolving $w(z)$ it is possible to lead to a case where this condition can be far from trivial to derive, mainly due to the integral in equation (3.3).

3.1 Parameterization of w_{de}

We will use the double kink parameterization of the dark energy equation of state in analogy to a single kink as described in the previous section. The idea is to test a second phase of acceleration that may take place at around $z = z_c$, and we

expect dark energy to be dominating at that redshift, as shown in Figure (3.1). Our parameterization has the form below

$$w_{de}(z) = w_0 + \frac{1}{2}(w_1 - w_0)\left[\tanh\left(\frac{z - z_1}{\Delta}\right) - \tanh\left(\frac{z - z_2}{\Delta}\right)\right], \tag{3.8}$$

where w_1 is the maximum value of the equation of state, and the transition width Δ. In this parameterization the easiest way to recover the ΛCDM case is to make $w_0 = w_1 = -1$ and the second term in the right hand side of equation (3.8) vanishes.

Using the parameterization (3.8) we can only evaluate $f(z)$ in equation (3.3) numerically and the condition for acceleration cannot be analytically found. In this section however as we are only concerned with the occurrence of another phase of acceleration after decoupling, we can set rough conditions for involved quantities for acceleration to happen (ρ_{de}, ρ_m, z) and make approximations. We know that for dark energy to dominate $\rho_{de} > \rho_m$ and using the simple constant w_{de} case ($f(z) = (1+z)^{3(1+w_{de})}$) we can have the condition that,

$$(1 + 3w_{de})(1 + z)^{w_{de}} > \frac{1}{\Omega_m^{-1} - 1}. \tag{3.9}$$

Clearly for $w_{de} > 0$ there is a high probability that ρ_{de} will dominate over matter and thus we have acceleration. In our parameterization w_1 represents the height of the step (see Figure (3.1)), then w_1 needs to be greater than zero for this condition to be fullfiled. In the future analysis where we will need not only acceleration but the best fit for current five year WMAP CMB power spectrum we will need to explore a much larger parameter space and therefore have to use an other approach. (see section (4.1)).

In Figure (3.1) we show our parameterization of w_{de} for some chosen parameter values, and we plot the evolution of the energy density for considered components namely dark energy and matter and compare the case with different values of w_1. We found that for higher values of w_1, DE tends to dominate earlier and stays dominating for a longer period than for low values of w_1. This implies that the acceleration phase starts earlier and stays longer in the case of high values of w_1 (see Figure (3.2)). We can see that at high redshift matter dominates over dark energy, it would be hard for dark energy to dominate unless it is given a very high

value of w_1. We also compared that evolution with the ΛCDM case ($w_{de} = -1$).

In Figure (3.1) we can see that in our parameterization, for w_{de} greater than zero and $\rho_{de} > \rho_m$, for some selected values, it is is possible to have a second phase of acceleration (see Figure (3.2)).

We could also parameterize w_{de} to have multiple kinks that will allow the two mentioned conditions to be satisfied and this would lead to multiple phases of acceleration. In the the following however we will limit our attention on the case of double kink only.

3.2 Preliminary test and comparison of our model against observations

In the previous section we tested the possibility of the second phase acceleration after decoupling. Now, we use selected parameter values for our double kink model, find the power spectrum, and compare it against WMAP observations. In our parameterization we investigate the effect in the power spectrum due to the change of values in redshift z_2, the w_1 parameter and the width of the transition Δ which will help in later analysis in our optimization. Figures (3.3) and (3.4) give more details.

We used the five years WMAP binned TT data (NASA (2008a)) (we will use the same data throughout this work) publically available, and the CAMB code (Lewis *et al.* (2000)) which we modified in order to be able to include it in our Monte Carlo approach (details in section (4.4)). Clearly the CMB powerspectrum is sensitive to any of the considered parameters as one would expect. In general the most affected part in the CMB power spectrum corresponds to low l which is the ISW part. Higher values of parameters z_2 and w_1 affect more the ISW plateau, what is not the case for the parameter Δ. The higher the values for parameter Δ, the less is the effect on the ISW plateau. This basically gives the idea that if one samples from a large parameter space there may be some chance of getting a good fit to the WMAP data. We carry a further analysis on this in the next chapter. To obtain Figure (3.3) and Figure (3.4), we used a matlab code in (B.4).

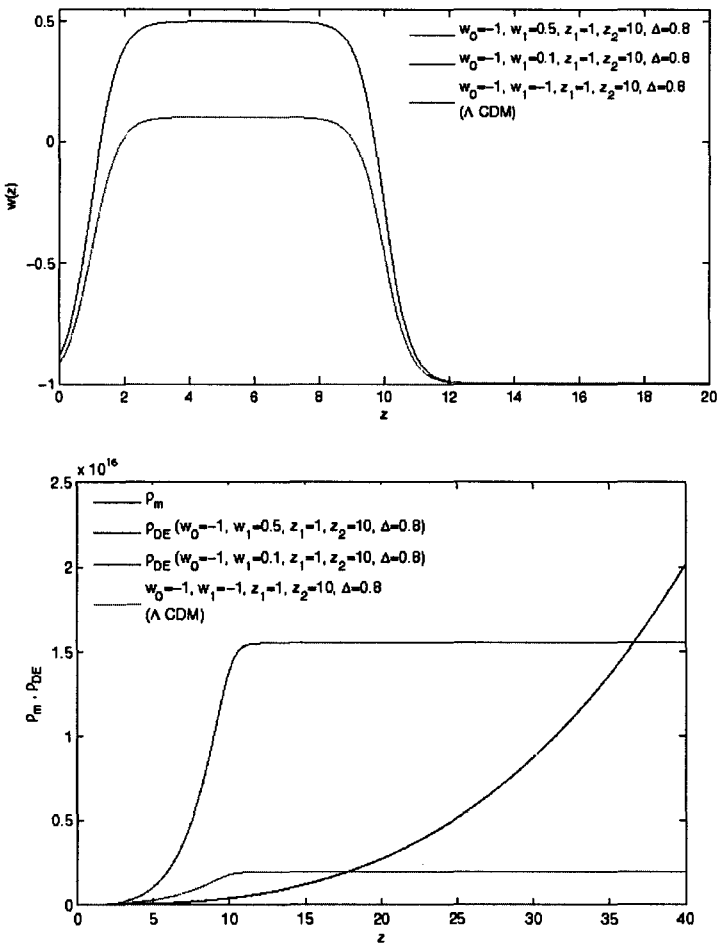

Figure 3.1: Top panel: $w_{DE}(z)$ *in the double kink parameterization for three set of parameters (note the third set which represent the* ΛCDM *case lies on* $w(z) = -1$ *line) considered including* ; bottom panel: $\rho_m(z)$ *and* $\rho_{DE}(z)$ *corresponding from our parameterization using the same set of parameters and* ΛCDM *case.*

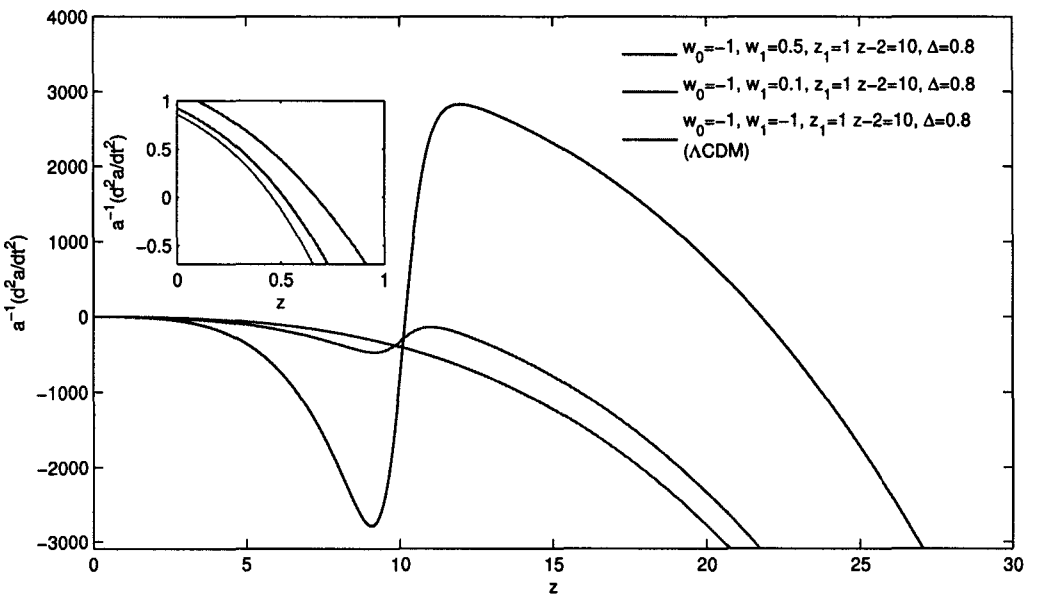

Figure 3.2: *$\ddot{a}/a$ plots corresponding to three particular cases in our parameterization using the same sets of chosen parameters as in Figure (3.1) .*

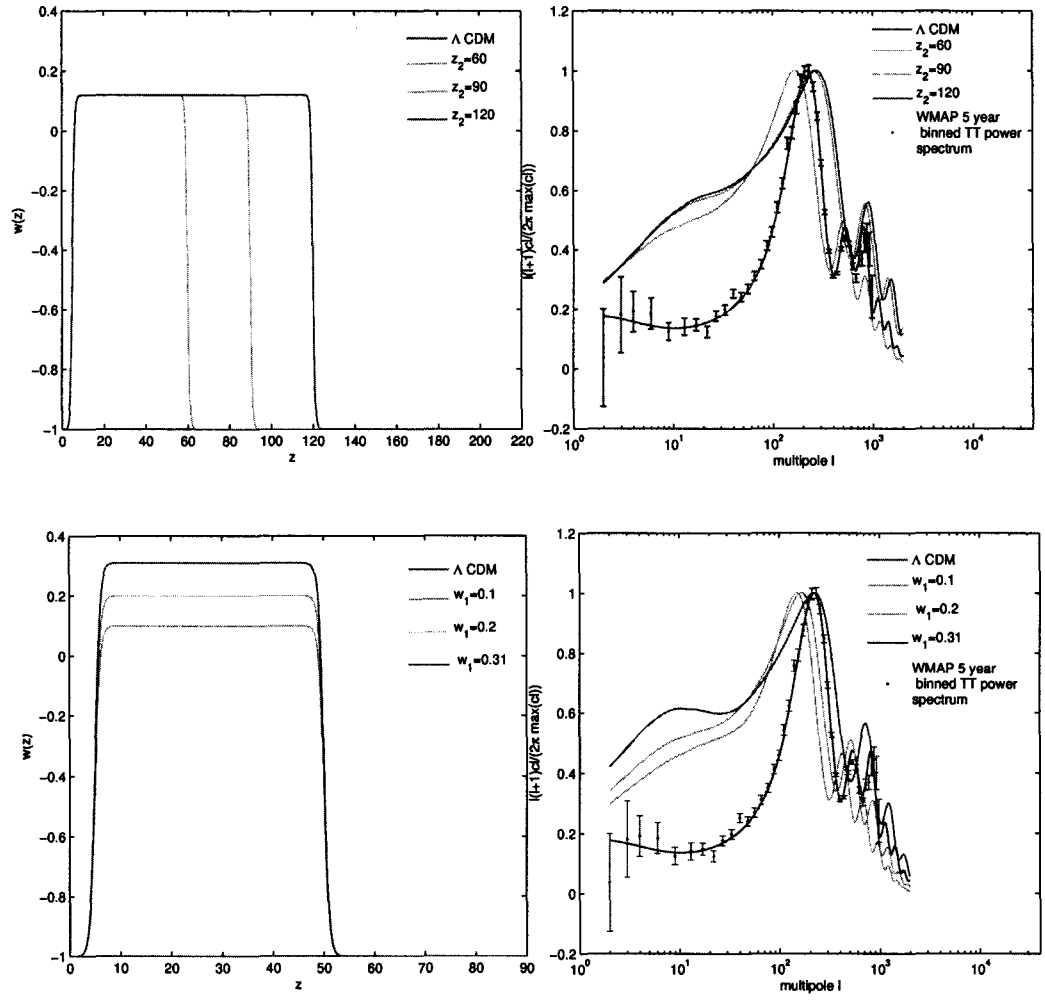

Figure 3.3: Top left panel:$w_{DE}(z)$ *in the double kink parameterization for five set of parameters by changing* z_2 *only,* top right panel: *obtained CMB power spectrum using the same set of parameters.* Bottom left panel: $w_{DE}(z)$ *in the double kink parameterization for five set of parameters by changing* w_1 *only,* bottom right panel: *Corresponding change in the CMB power spectrum. In all cases we also considered* ΛCDM *case to make comparison and for the power spectrum were fitting WMAP 5 year binned TT data (dots with errorbars).*

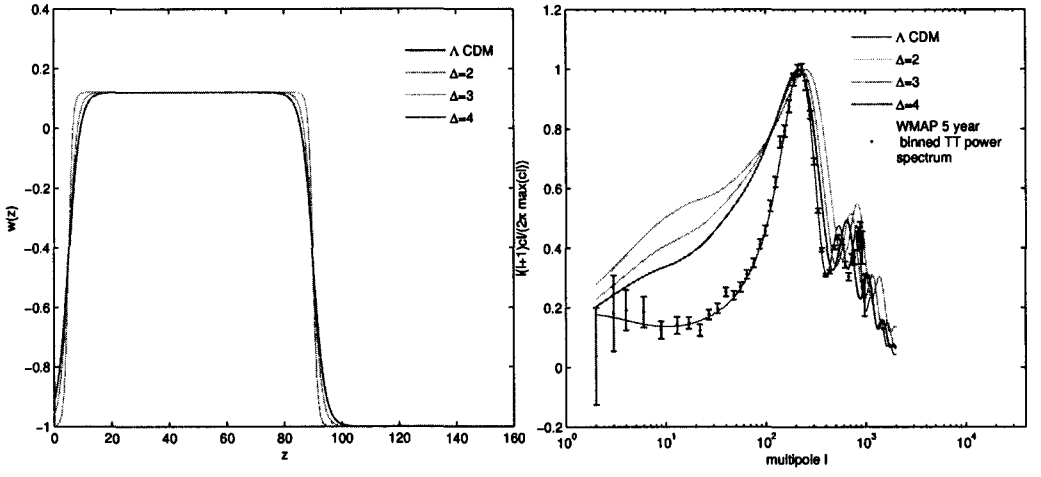

Figure 3.4: Left panel: $w_{DE}(z)$ *in the double kink parameterization for four set of parameters by only changing* Δ, right panel: *Corresponding change in the CMB power spectrum. We also considered* ΛCDM *case to make comparison and for the power spectrum were fitting WMAP 5 years binned TT data (dots with errorbars).*

Chapter 4

Searching for a second phase of acceleration

The previous analysis is clearly lacking robust sampling for exploring our parameter space. However, we showed that it is a possible to get more than one phase of acceleration after decoupling with some chosen values in our parameterization. In this chapter we will use a modified Markov Chain Monte Carlo (MCMC) approach and allow much larger spatial variability for our parameter space (see section 4.4 for more details) . We will use WMAP data in computing the statistical quantities like χ^2 and the Likelihood in this approach. In the previous chapter, we naively estimated the condition for acceleration. We now use all the 5 parameters in the double kink parameterization, and in addition to just testing for acceleration, we will determine whether those parameters yielding acceleration are a good fit to the CMB TT power spectrum from WMAP data. In the next section we derive a new acceleration condition taking into account our parameterization, in section (4.2) we describe the parameter space we sample over, sections (4.3, 4.4) discuss briefly our statistical approach based on Bayesian inference and in section (4.5) we describe our results.

4.1 Condition for acceleration

For a double step function constant w_{de}, one can derive analytical simple expression for $f(z)$, and obtain an approximated condition for acceleration. In this case

we write

$$w_{de}(z) = \begin{cases} w_0\,, & z < z_1 \\ w_1\,, & z_1 < z < z_2 \\ w_0\,, & z > z_2 \end{cases} \tag{4.1}$$

This yields an $f(z)$ (different from the constant case considered in the previous chapter), obtained using equation (3.3)

$$f(z) = \begin{cases} (1+z)^{3(1+w_0)} & \text{when } z < z_1 \\ (1+z_1)^{3(1+w_0)} \left(\frac{1+z}{1+z_1}\right)^{3(1+w_1)} & \text{when } z_1 < z < z_2 \\ (1+z_1)^{3(1+w_0)} \left(\frac{1+z_2}{1+z_1}\right)^{3(1+w_1)} \left(\frac{1+z}{1+z_2}\right)^{3(1+w_0)} & \text{when } z > z_2 \end{cases} \tag{4.2}$$

We need to derive the constraints we should put on any of the above parameters in order to get acceleration using the form of $f(z)$ above. The condition on z_2 for having acceleration can be obtained by using the above result at z_2

$$f(z_2) = (1+z_1)^{3(1+w_0)} \left(\frac{1+z_2}{1+z_1}\right)^{3(1+w_1)}, \tag{4.3}$$

and the acceleration condition (3.7). Combining these we reach

$$(1+z_1)^{3(1+w_0)} \left(\frac{1+z_2}{1+z_1}\right)^{3(1+w_1)} (1+w_0) < \frac{\Omega_{m0}(1+z_2)^3}{\Omega_{m0}-1}, \tag{4.4}$$

which yields the condition for z_2 in terms of parameters Ω_{m0}, w_0, w_1, and z_1

$$z_2 > z_{2,min} = \left[\frac{\Omega_{m0}}{\Omega_{m0}-1}\frac{1}{1+w_0}\right]^{1/3w_1} (1+z_1)^{\frac{w_1-w_0}{w_1}} - 1. \tag{4.5}$$

This relation gives the minimum value $z_{2,min}$, that z_2 must take for acceleration to take place. However, we also need to take into account the transition width Δ which is zero in the double step-function approximation but has some non-zero values in our actual parameterization (3.8). We want to improve the step function by introducing a transition width. However deriving a bound like (4.5) with a non-zero width Δ does not seem analytically tractable. Furthermore, for numerical implementation, to guarantee stability in long MCMC chains, we choose a minimum value between $max(z_1, \beta z_{2,min}, z_{2,n})$ and z_{max}; where $z_{2,n} = z_{2,n-1} + \delta z_2$ is the value obtained after incrementing a proposed z_2 value $z_{2,n-1}$ by δz_2 (obtained through the Metropolis Hastings algorithm described in section (4.4)) with

δz_2, z_{max} a maximum value that z_2 is allowed to take and β a coefficient to soften the bound (4.5) so that we don't exclude a desired model. In our analysis we used four values of β: 0.56, 0.8, 0.91 and 1.2. We set $z_{max} = 1100$ as we are only interested in the post-decoupling epoch.

The condition derived here is just an approximation and all the obtained z_2 values may not always lead to acceleration. We tested this condition in five chains of 50,000 steps in totally generated by random steps that satisfy condition in relation (4.5) from a chosen initial position. We found that all steps proposed using this condition lead to an acceleration phase at some redshift z_c and that the higher the values of β the higher the probability for getting acceleration. Figure (4.1) shows the obtained acceleration of 20 randomly selected steps from the produced chains. This shows that in addition to the current acceleration phase we have

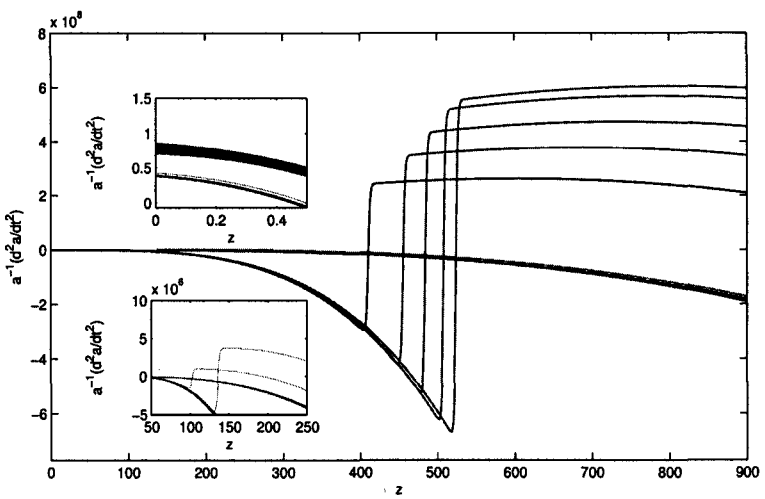

Figure 4.1: *ä/a plots for 20 randomly selected steps in one of the output test chains obtained using* $\beta = 0.56$.

another acceleration phase starting at some redshift where $\ddot{a} > 0$.

4.2 Cosmological parameters

The adiabatic cold dark matter (CDM) model basically relies on 13 parameters. These include the Hubble parameter H, the scalar and tensor spectral index n_s and n_t, scalar and tensor perturbation amplitudes A_s and A_t, the tensor to scalar ratio r, the running of the scalar tilt α, the reionization optical depth, τ, dark matter, baryon, neutrino, DE, curvature energy densities $\Omega_c, \Omega_b, \Omega_n, \Omega_{de}, \Omega_k$ respectively (Dunkley *et al.* (2009)). However, we only consider 6 free parameters out of those in our sampling, which are more susceptible to affect dark energy the most namely, Ω_{de}, Ω_b, Ω_c, H, τ, and n_s.

For our total sampling space, we also consider 5 parameters for the double kink parameterization of the equation of state parameterization w_0, w_1, z_1, z_2 and Δ. We will then be sampling over an 11 parameter space that we can divide into two main parts: 5 free dark energy equation of sate parameters and 6 free cosmic parameters, that can be represented in vector space as

$$\vec{p} = (w_0, w_1, z_1, z_2, \Delta, H, \Omega_b, \Omega_c, \Omega_{de}, \tau, n_s). \tag{4.6}$$

The remaining parameters are left fixed to their ΛCDM best fit values (NASA (2008c)). There are already known constraints on ΛCDM model using five -year WMAP data. The constraints depend on which set of parameters are chosen. In panels (4.2) are showing constraints on different parameters for ΛCDM case.

4.3 Likelihood Analysis

Assuming that D represents all the data points, and a parameter space with m parameters

$$\vec{\Theta} = (\Theta^{(1)}, \Theta^{(2)}, ..., \Theta^{(m)}) \tag{4.7}$$

if we randomly sample over the parameter space $\vec{\Theta}$, the likelihood $L(\vec{\Theta})$ is fundamentally defined as the probability distribution function (PDF) of D containing the data given the parameter space $\vec{\Theta}$ and priors on the parameters, usually denoted as $P(D|\vec{\Theta})$ which is a conditional PDF. Then if the likelihood function of a certain parameter vector $\Theta^{(1)}$ is higher than the likelihood function of parameter vector $\Theta^{(2)}$ then $\Theta^{(1)}$ is retained as more plausible and observations under $\Theta^{(1)}$ are more likely than observations under $\Theta^{(2)}$. Although $P(D|\vec{\Theta})$ is relatively easy

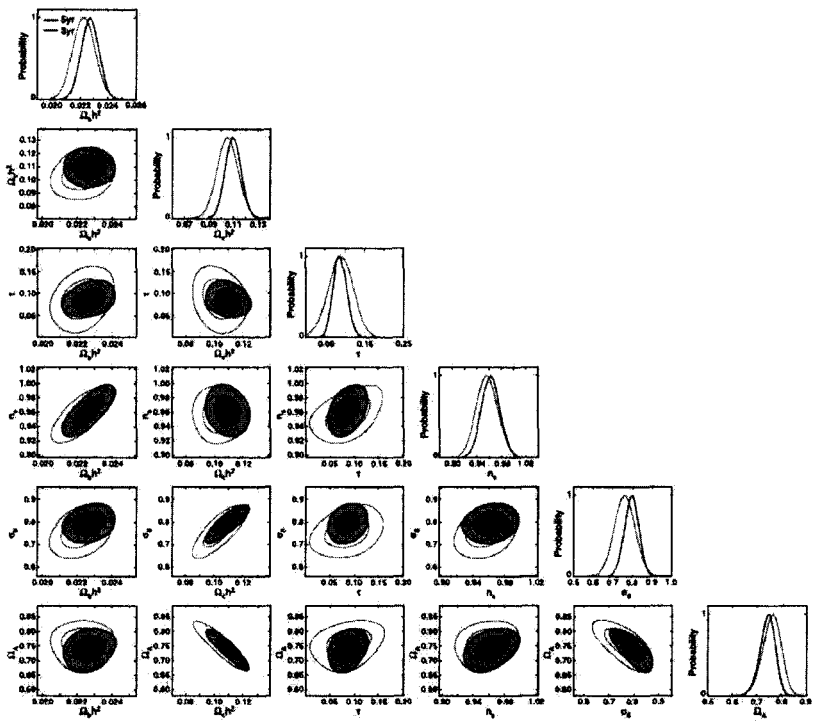

Figure 4.2: *Marginalized one- and two-dimensional distributions within* 68%*(inner contours) and* 95%*(outer contours) for five-year(blue) and three-year(grey) WMAP TT power spectrum constraints on* ΛCDM *parameters* (Dunkley *et al.* (2009)).

to find, in general the needed information is through the quantity which would allow us to find the unknowns which are the parameters. This is done by finding the posterior conditional probability $P(\vec{\Theta}|D)$ which is related to the likelihood through Bayes' theorem as

$$P(\vec{\Theta}|D) = \frac{P(D|\vec{\Theta})P(\vec{\Theta})}{N(D)}, \tag{4.8}$$

where $P(\vec{\Theta}|D)$ is called the posterior distribution, $P(\vec{\Theta})$ is the prior probability distribution, representing the degree of belief one has before observing the data, $N(D) = \int P(D|\vec{\Theta})P(\vec{\Theta})d\vec{\Theta}$ is the marginal PDF of D. As $N(D)$ is independent

of $\vec{\Theta}$, it can be regarded as the normalization constant, and equation (4.8) reduces to

$$P(\vec{\Theta}|D) = P(D|\vec{\Theta})P(\vec{\Theta}) \tag{4.9}$$

The only way to extract information about one parameter like $\Theta^{(\iota)}$, is through marginalization where one has to perform an $(m-1)$- dimension integral over other parameters $\Theta^{(k\neq\iota)}$ with $k = 1, ..., m$, and its expectation value is obtained by integrating the individual posterior PDF. In practice, due to the case of high dimension space it almost unavoidable to use a sampling method for the posterior PDF.

In general, parameters can be extracted due to the fact that in the case of Gaussian errors, one can build a likelihood function from the data D via the expression

$$L(\vec{\Theta}) \propto \exp - \left(\frac{1}{2}(D-\Theta)^T[C_{\vec{\Theta}}]^{-1}(D-\Theta)\right), \tag{4.10}$$

where $C_{\vec{\Theta}}$ is the data covariance matrix and $(D-\Theta)^T$ is the transpose of $D-\Theta$. In most cases it is assumed that data points are independent; then the covariance matrix is diagonal and equation (4.10) is approximated to be

$$L \propto \exp\left(-\chi^2/2\right), \tag{4.11}$$

with

$$\chi^2 = \sum_{l}^{S} \left(\frac{C_l^d - C_l^t}{\sigma(C_l)}\right)^2, \tag{4.12}$$

where C_l^d is the measured value, C_l^t is the theoretical value obtained from a model, $\sigma^2(C_l)$ is the variance of data or error in data, and S is the total number of data points.

Equation (4.10) establishes the link between the posterior PDF of the parameters and the experimental data. The main issue here for extracting parameters is trying to minimize χ^2 (or maximize the likelihood L) which in practice can be very complicated as the likelihood space can have multiple minima. There are a lot of ways for getting to the global minimum which in that case becomes an optimization problem (Andrieu *et al.* (2003)). If the likelihood function is a continuous differentiable equation, the optimization is determined by the possibility to find gradient of χ^2, but in multidimensional case, one needs a more robust algorithm for finding the global minimum. One powerful method to do deal with that is

using Monte Carlo techniques that we briefly describe in the following section. For a more substantial coverage of the subject, the reader is referred to Spall, James C. (2003).

4.4 Markov Chain Monte Carlo (MCMC) Sampling

Markov chain is an example for stochastic systems (discrete or continuous) relying on a transition probability T such that from the PDF of the current point in the parameter space $\vec{\Theta}_i$, is drawn from the PDF of the new proposed point $\vec{\Theta}_{prop}$, i.e. $T(\vec{\Theta}_{prop}|\vec{\Theta}_1, ..., \vec{\Theta}_i) = T(\vec{\Theta}_{prop}|\vec{\Theta}_i)$. Assuming that all the points can be reached, T leaves the distribution invariant and the chain distribution asymptotically tends to the posterior distribution.

One common way of constructing a Markov chain is via the Metropolis-Hasting (MH) algorithm (Hastings (1970); Metropolis *et al.* (1953)). This uses the MCMC method to sample the Markov chain for long enough in order to allow the chain to reach the equilibrium. The obtained chain can be used as the sample from the posterior PDF. The main points of the MH algorithm is the rejection or acceptance of the proposed step $\vec{\Theta}_{prop}$ which depends on the current step $\vec{\Theta}_i$ via

$$\alpha(\vec{\Theta}_{prop}, \vec{\Theta}_i) = \min\left\{1, \frac{P(\vec{\Theta}_{prop})q(\vec{\Theta}_i|\vec{\Theta}_{prop})}{P(\vec{\Theta}_i)q(\vec{\Theta}_{prop}|\vec{\Theta}_i)}\right\}, \tag{4.13}$$

with q an arbitrary proposal distribution function. Different $\vec{\Theta}_i$ are candidate points from q. α gives the probability for the proposed state to be accepted. The transition probability is then given by

$$T(\vec{\Theta}_{i+1}|\vec{\Theta}_i) = \alpha(\vec{\Theta}_{i+1}, \vec{\Theta}_i)q(\vec{\Theta}_{i+1}, \vec{\Theta}_i). \tag{4.14}$$

If the proposal distribution $q(\vec{\Theta}_{prop}, \vec{\Theta}_i)$ is chosen to be symmetric, the relation (4.13) becomes

$$\alpha = \min\left\{1, \frac{P(\vec{\Theta}_{prop})}{P(\vec{\Theta}_i)}\right\} \equiv \min\left\{1, \frac{L(\vec{\Theta}_{prop})}{L(\vec{\Theta}_i)}\right\}. \tag{4.15}$$

This relation just involves the ratio of the posterior distribution, and this is the major advantage, particularly for Bayesian approach where the normalization factor in equation (4.8), normally hard to compute, is no longer an issue; and one can compute the posterior distribution from the likelihood of the data and the priors.

It is important to note that MH algorithm can be considered as a sample from the invariant density only after a certain number of steps in the chain. Those steps would correspond to the period when the chain started to converge which happens after so called *burn-in* period. Convergence diagnostics have been developed in order to ensure that the produced chains really are the representative of the initial distribution (Gelman *et al.* (1996), Roberts & Tweedie (1996)).

Proposal distribution and choice of priors

A Proposal distribution q gives samples from the target distribution P. For more general discussion see (Gelman *et al.* (1996), Roberts & Tweedie (1996), Mengersen & Tweedie (1996)). In this work limit ourselves on symmetric q, and we use equation (4.15) to compute the acceptance probability. We obtain the proposed step Θ^{ι}_{prop} via

$$\Theta^{\iota}_{prop} = \Theta^{\iota}_{i} + \sigma_{\iota}.x \equiv \Theta^{\iota}_{i} + \delta\Theta^{\iota}, \tag{4.16}$$

where x is a random number obeying a gaussian distribution centered on zero with unit variance, and $\delta\Theta^{\iota}$ is the increment for each parameter.

In practice one has to be careful in choosing σ_{ι}. Small steps $\vec{\Theta}_{i+1} - \vec{\Theta}_{i}$ would lead to a high acceptance ratio but the chain will take a long time to reach interesting region; on the other hand large steps $\vec{\Theta}_{i+1} - \vec{\Theta}_{i}$ would also generate a low acceptance probability i.e. very small α. This would lead to a low acceptance and a long correlation length. Ideally the two extreme can be avoided by scaling the proposal distribution and dynamically adjusting parameters. Knowing how sensitive, fast or slow a parameter is, can help to decide whether one has to choose simple (linear), or nonlinear proposal distributions. Then for a particular problem the priors have to be chosen carefully along with their ranges.

A typical MCMC algorithm

The MCMC sampler using the MH algorithm is based on the following steps (also one can check the flowchart (B.1) :

- Start at a random position $\vec{\Theta}_0$ within the range given by priors
- Compute the quantity $L_0 = P(D|\vec{\Theta}_0)$ using equation (4.11)
- Loop over the index i until $i = Nsim$ where the chain is expected to be long enough and has converged.

  a) By specifying the variance for each parameter σ_ι, obtain the proposed parameter values via $\Theta^{(\iota)}_{prop} = \Theta^{(\iota)}_i + \sigma_\iota.x$, where x is a random number obeying a Gaussian distribution.

  b) Compute the quantity $L_{prop} = P(D|\vec{\Theta}_{prop})$ using equation (4.11)

  c) Calculate the ratio $r = L_{prop}/L_i$

  d) If $r > 1$, then set $\vec{\Theta}_{i+1} = \vec{\Theta}_{prop}$

  e) Else, sample from a uniform distribution $U \in (0, 1)$

$$if \begin{cases} r > U & \text{set } \vec{\Theta}_{i+1} = \vec{\Theta}_{prop} \text{ accepted} \\ r < U & \text{set } \vec{\Theta}_{i+1} = \vec{\Theta}_i \text{ rejected} \end{cases} \tag{4.17}$$

4.5 Modified MCMC and optimization

In this section we describe our parameter space and how much we were able to explore it in this work. We also give some details on how we searched for the best fit parameters for the CMB power spectrum.

4.5.1 Parameters and priors

As described in previous sections, our work is based on an 11 free parameters that we can divide into two categories: dark energy parameters through the double kink model $w_0, w_1, z_1, z_2, \Delta$ and cosmological parameters $H_0, \Omega_b, \Omega_c, \Omega_{de}, \tau, n_s$. We computed the CMB TT power spectrum using a modified version of CAMB (Lewis *et al.* (2000)) which we found to be faster than the modified CMBfast (Zaldarriaga & Seljak (2000)) version that we had started with. The main issue

in the analysis is the implementation of the condition for acceleration for one parameter given the rest.

Referring to the work in Bassett *et al.* (2004) dark energy parameters used don't introduce new degeneracies with normal ΛCDM parameters, but can be degenerate within themselves. This may be for instance the case for z_1 and z_2 as they are correlated. On the other hand there are several known degeneracies amongst the base cosmological parameters used (eg: n_s and Ω_b; τ and n_s, Ω_c, H_0); it is thus necessary to consider all of those as well as previous constraints on dark energy parameter (Bassett *et al.* (2002)) for a better choice of priors. In this work our main objective is to produce as many chains as possible based on the MH algorithm and then using WMAP five year TT power spectrum extract the minimum χ^2, χ^2_{min} from the chain corresponding to the maximum likelihood. We expect that to be also the good fit of the data if it is comparable with the WMAP best fit reduced χ^2. In this case as we are only interested in optimization, and because we are also starting our chains to the region closer to currently known best fit for the six cosmological parameters, considering the burn-in period is not even necessary.

In our analysis we were obliged to impose an extra-condition (4.5) while sampling over parameter z_2 due to the double step approximation to our double kink parameterization. This then modifies the standard MCMC (see (4.4)). Due to this condition we also have output chains with low acceptance rate, at least in the region we were able to explore. We produced in total 5 chains making 120,000 steps in total (30,000+30,000+30,000+20,000+10,000) using different priors for each. The reason for this is that we wanted to explore as much posterior space as possible to try and pinpoint the minimum χ^2. For all parameters we chose a linear space with constant step σ_i except for z_1 and z_2 where we assumed that $z_2 > z_1$ and considered their steps should increase via the relation $\sigma_i = \sigma_i(1+z_{pi})$), where σ is the standard deviation and z_p a proposed new step, in order to make sure that at high redshift we allow longer jumps, what would increase the chance of detecting DE domination. In table (A.2) below we show our parameters and considered prior ranges for 2 chains out of 5 generated. The rest of the chains can be found in appendix (A.1).

The implementation of this modified MCMC method for optimization can be far from trivial when one has to deal with high dimensional space. Many correlations

Table 4.1: Free parameters and corresponding priors for 2 first generated chains.

Free parameters range	Chain 1:start,σ	Chain 2: start, σ
-1.0< w_0 < -3×10^{-1}	-0.946, 8×10^{-4}	-0.854, 8×10^{-3}
0< w_1 < 9×10^{-1}	0.283, 8×10^{-4}	0.301, 8×10^{-3}
5×10^{-1} < z_1 <850	15, 1.08	20, 1.2
5×10^{-1} < z_2 <850	105, 1.01	125, 1.2
1.6 < Δ <4	2.4, 6×10^{-3}	1.8, 4×10^{-3}
40< H_0 <100	64.2, 1.2	75.3, 1.6
$4 \times 10^{-3} < \Omega_c < 1.5 \times 10^{-1}$	2.34×10^{-1}, 4×10^{-3}	0.228, 6×10^{-3}
$6 \times 10^{-2} < \Omega_b < 6 \times 10^{-1}$	4.1×10^{-2}, 1.5×10^{-3}	$0.045, 1.7E-3$
$2 \times 10^{-1} < \Omega_{de} < 9 \times 10^{-1}$	0.601, 4.2×10^{-3}	0.741, 5.7×10^{-3}
$4 \times 10^{-2} < \tau < 10^{-1}$	0.072, 2.4×10^{-3}	0.086, 1.6×10^{-3}
$3 \times 10^{-1} < n_s < 1.2$	0.780, 7.9×10^{-3}	0.85, 8.1×10^{-3}

are inevitable, and this can lead to a high rejection rate.

Priors were chosen to efficiently explore space. We determined different sensitivities of used parameters by averaging over all the steps for each parameter and then comparing with their minimum values. We found that parameter $H_0, \Omega_c, \Omega_b, \Omega_{de}$ are less sensitive than $n_s, \tau, w_0, w_1, z_1, z_2, \Delta$, which is also related to how fast they can change. In different runs of the code we made we had values of some of the parameters that may limit us in exploring more space as we wanted. For instance values of $w_1 \gtrsim 0.3$ usually lead to no power spectrum output in the CAMB due to the divergence in the Rombint integral needed to obtain the power spectrum (Bashinsky & Bertschinger (2002)). It also was found that the CMBfast code has problems giving the results in the case of a small transition width $\Delta \lesssim 0.4$ and the instabilities can also lead to some error messages. We then had to choose prior ranges taking into account those issues. One advantage of using MCMC like approach is that the computational demands of Bayesian inference with a large number of parameters is well met and there is no need to calculate the integral for the normalization constant. It is also easy to handle the marginalization of parameters by just considering the steps of one parameter in each chain.

We made the main run of our code at the South Africa Center of High Performance Computing (CHPC), on an IBM e1350 Cluster which is an iQudu machine. In Figures (4.3) and (4.4) are shown the histograms respectively for equation of state parameters and cosmic parameters. This represents the explored space as well as the region of high or low acceptance rate by referring to the height and width of boxes in histograms. Due to imposed condition for z_2 to get the acceleration phase, the acceptance rate was even $< 5\%$ in some chains. For dark energy parameters the z_1 is not well sampled mainly due to the condition for acceleration (4.5), There is almost no value in the region corresponding to $w_1 > 0.3$ because mostly no output from the used CAMB code.

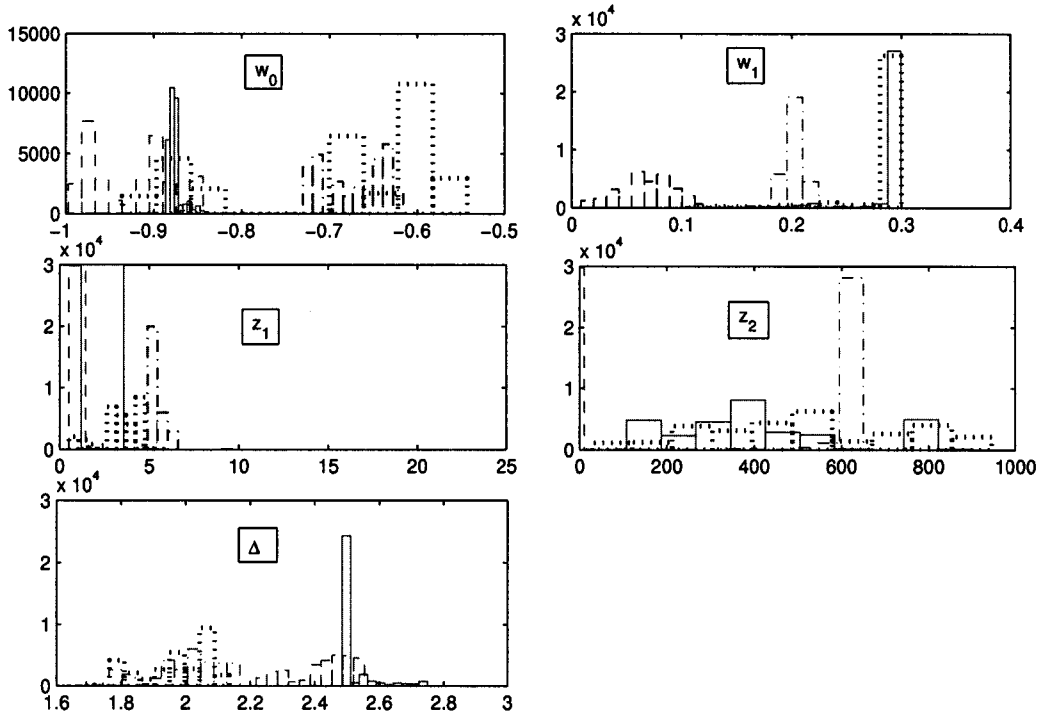

Figure 4.3: *Histograms for 5 parameters(w_0, w_1, z_1, z_2 and Δ) from 5 produced chains:* red broken line, green broken, magenta solid line and dotted line, *from the first to the third chain respectively*, the last two are in black dotted line.

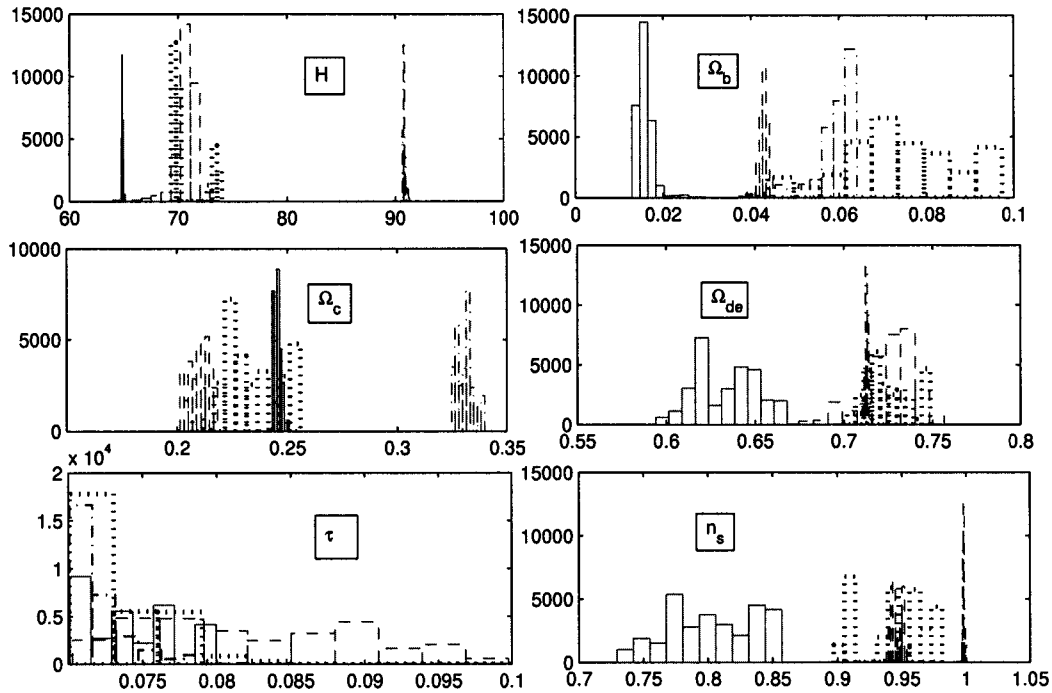

Figure 4.4: *Histograms for 6 parameters(H, Ω_b, Ω_c, Ω_{de}, τ and n_s) from four of produced chains:* red broken line, green broken, magenta solid line and dotted line, *from the first to the third chain respectively*, the last two are in black dotted line.

4.5.2 Probing the acceleration phase and CMB power-spectrum best fit

From the chain produced we also computed and plotted the chi-squared per degree of freedom distribution in each chain and the compared them. The minimum obtained χ^2 value was 1.98 from the first chain. See Figure(4.5).
We used a matlab code (See appendix B.2) for selecting models within a range ± 0.9 of a χ^2 per degree of freedom (p.d.o.f) of 1. We then computed the acceleration for those best fit parameters and the corresponding CMB power spectrum using the CAMB code. In all chains we produced we found those steps having a χ^2 p.d.o.f falling in that range, there is no second phase of acceleration detected

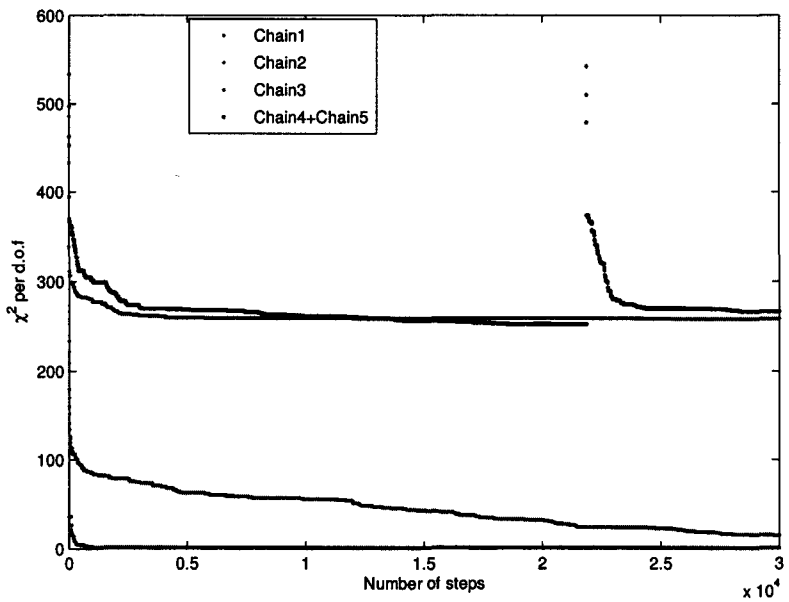

Figure 4.5: *Plot comparing the χ^2 per degree of freedom (p.d.o.f) from all the five chains. A cut and peak in one of the curves is due to the two last combined chains (chain 4 plus chain 5).*

as shown in Figure (4.6). In all chains, the χ^2 p.d.o.f decreases with the number of steps. This is mainly due to MH test and it shows that we are on a good track for the minimum χ^2 and hence the best fit. The best of our five chains is chain number 1 with the smallest χ^2. We see that the steps which yield a decent fit to the data do not have a second phase of acceleration, implying that we were unable to simultaneously fit the WMAP data and have have multiple phases of acceleration.

It is worth reminding that we only probed a limited region of parameter space as indicated in Table (A.2) and that we only produced a total chain length of 120,000 steps. Our analysis was also based to an approximation of our actual parameterization for obtaining the acceleration condition. In addition the codes used like CAMB only provides, for the parameterization used, an output for only up to a certain value of $w_1 \lesssim 0.3$. Taking into account those limitations, we can say that our search results don't necessarily lead to the exclusion of the

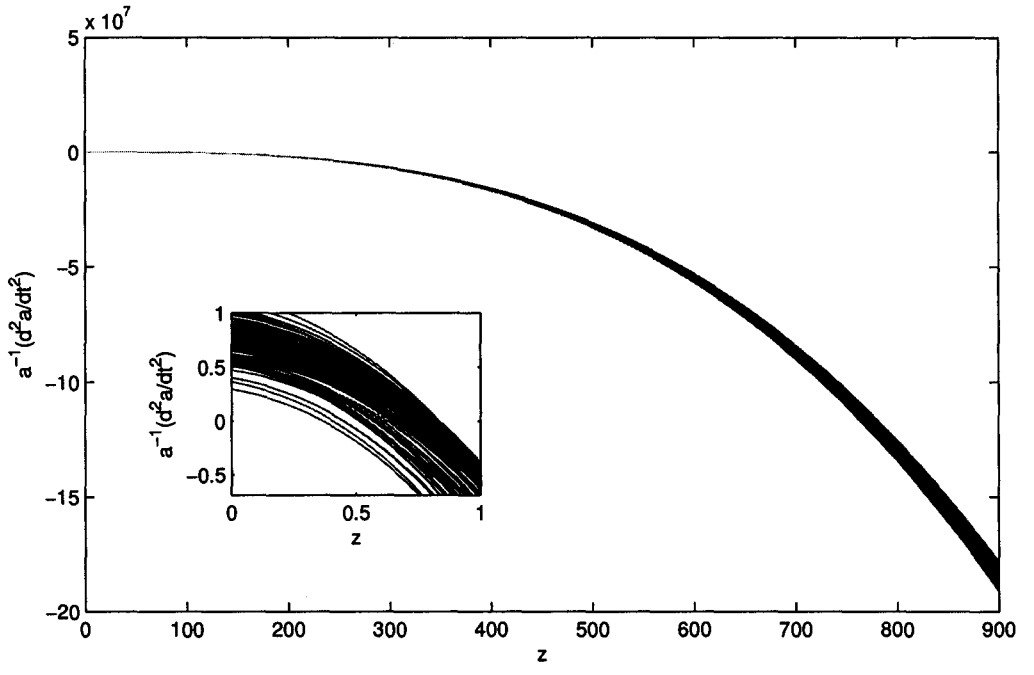

Figure 4.6: $\ddot{a}/a$ *plots for models with* χ^2 *p.d.o.f* < 1.9.

possibility that there are models which simultaneously fit the ΛCDM data and yield a second phase of acceleration even in the parameter region set by our priors.

In this search we focused on models with acceleration i.e., fulfilling the acceleration condition (4.1) while being a good fit to the current CMB data. We restrict ourselves on quintessence case (i.e. we only consider that the speed of sound of dark energy to be 1). This restricts our search to only scalar field models, which we also think limits the number of models with second phase of acceleration.

In the modified MCMC used we impose that condition and sample over our parameter space. The parameter β introduced allows the smoothing of the double step function used as an approximation to our double kink parameterization. Different values of β and models with a speed of sound different from unity would be interesting extensions of the work presented here. They are left for future study.

Chapter 5

Conclusions

In this work we investigated a possible second phase of acceleration since decoupling using a double kink parameterization of the equation of state. In Chapter 1 we introduced the the main purpose of this work. In Chapter 2 we gave a short introduction to cosmology; in Chapter 3 we described the parameterization used and its main impact on the current CMB data. We also showed that the equation of state can play an important role in starting the acceleration phase. In the previous Chapter we derived the acceleration condition that we obtained by approximating the double kink parameterization of the DE $w_{de}(z)$ to a step function and a parameter β accounting for a non-zero transition width. A modified MCMC sampling tool is used to optimize the search for those parameters that can lead to the acceleration phase and also fit CMB data.

Our explored space was confined by different constraints as we discussed in the last chapter. For instance, the CAMB code couldn't give output for high values of w_1 which we would expect to have a great impact in leading to acceleration easily as mentioned in Chapter 3. We also only used limited number of values of β as the code was computationally expensive (almost a week to produce a chain of 30000 steps long). In the explored space with 120,000 steps in total, we find no models that simultaneously fit the WMAP data and yield a second phase of acceleration, as shown in our χ^2 analysis. This however doesn't exclude totally the plausibility of second phase of acceleration due to the limited parameter space probed. It is also worth noting that we just used one form of parameterization of the equation of state, which also constrains our results.

This work also treated dark energy as quintessence and we set the dark energy sound speed to be one, which implies that our search only involved scalar field models with negligible fluctuations, and all models ruled out in this study are of such class. We suggest that in future the optimization should be done in regions that we were not able to explore. Longer chains would bring additional (although never conclusive since there is a small chance very rare models exist which are good fits) evidence for our main conclusion. Future extensions could include the exploration of different values of β as well as the study of classes of dark energy other than quintessence based on standard scalar fields. These would allow for dark energy speed of sound different from unity and hence clustering in the dark energy on small scales, which could potentially change our main conclusions.

Appendix A

A.1 Tables

Table A.1: Table showing priors used for the third chain.

Free parameters range	Chain 3: start,σ
-1.0< w_0 < -3×10^{-1}	-0.736, 3×10^{-3}
0< w_1 < 9×10^{-1}	0.109, 3×10^{-3}
5×10^{-1} < z_1 <850	37, 1.5
5×10^{-1} < z_2 <850	157, 1.5
1.6 < Δ <4	2.9, 3×10^{-3}
40< H_0 <100	81.5, 1.9
$4 \times 10^{-3} < \Omega_c < 1.5 \times 10^{-1}$	0.19, 1.2×10^{-3}
$6 \times 10^{-2} < \Omega_b < 6 \times 10^{-1}$	0.47, 1.9×10^{-3}
$2 \times 10^{-1} < \Omega_{de} < 9 \times 10^{-1}$	0.852, 2.1 $\times 10^{-3}$
$4 \times 10^{-2} < \tau < 10^{-1}$	0.089, 1.92×10^{-3}
$3 \times 10^{-1} < n_s < 1.2$	0.94, 1.2×10^{-2}

Table A.2: Table showing priors used for the fourth and fifth chains

Free parameters range	Chain 4:start,σ	Chain 5:start,σ
-1.0< w_0 < -4×10^{-1}	-0.623, 3×10^{-4}	-0.723, 3×10^{-4}
0< w_1 < 9×10^{-1}	0.079, 3×10^{-4}	0.219, 3×10^{-4}
5×10^{-1} < z_1 <850	15, 1.08	15, 1.08
5×10^{-1} < z_2 <850	135, 1.01	105, 1.01
1.6< Δ <4	2.01, 6×10^{-3}	2.04, 6×10^{-3}
40< H_0 <100	91.01, 1.2	73.01, 1.2
$4 \times 10^{-3} < \Omega_c < 1.5 \times 10^{-1}$	3.1×10^{-2}, 4×10^{-3}	3.9×10^{-2},4×10^{-3}
$6 \times 10^{-2} < \Omega_b < 6 \times 10^{-1}$	3.4×10^{-1},1.5×10^{-3}	3.8×10^{-1},1.5×10^{-3}
$2 \times 10^{-1} < \Omega_{de} < 9 \times 10^{-1}$	6.1×10^{-1}, 4.2×10^{-3}	5.6×10^{-1}, 4.2×10^{-3}
$4 \times 10^{-2} < \tau < 10^{-1}$	8.2×10^{-2}, 2.4×10^{-3}	7.5×10^{-2}, 2.4×10^{-3}
$3 \times 10^{-1} < n_s < 1.2$	7.3×10^{-1}, 7.9×10^{-3}	7.9×10^{-1}, 7.9×10^{-3}

Appendix B

B.1 Typical MCMC flowchart

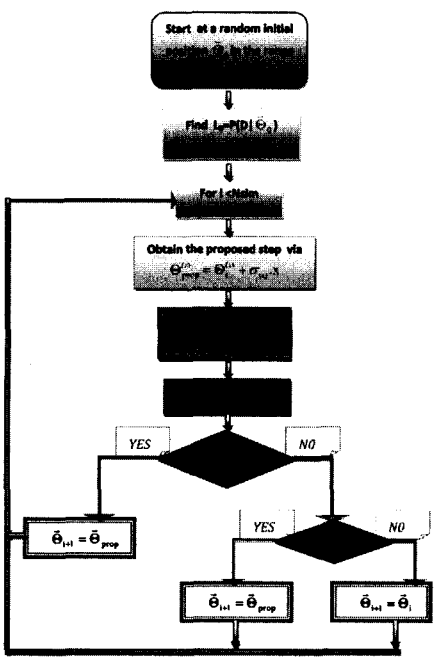

Figure B.1: Flowchart of a typical MCMC based on Metropolis Hastings algorithm.

B.2 MCMC Code

```
 ! ------------------------
!a) program MCMCAMB !MCMC code
! ------------------------

! This f77 program uses Monte Carlo Markov Chain(MCMC) sampling
!       technique to generate chains of parameters in a specific Model.
!        Our Model uses double-KINK to parameterize the equation of state w(z)
! w(z)=w0+0.5(w1-w0)[(tanh((z-z1)/delta))-(tanh((z-z2)/delta))] with 5
!       parameters:
! w0:The equation of state value now(redshift z=0)
! w1: The equation of state value at some redshift z
! z1: The redshift of transition (2nd)
! z2: The redshift of transition (1st)
! delta: The transition width.
! The Chi-Squared is generated through the CAMB code
! (TT CMB power spectrum )and the WMAP 5 years binned TT
!       power spectrum. The loglikelihood corresponding to the
! sampled parameter values at each step are also given.
! INPUTS:
! a)Files:
! -Initial parameter file:'wzparams.txt~'
! -WMAP 5 years binned TT power spectrum file:
!        'wmap_binned_tt_spectrum_5yr_v3.txt'
```

```
! -Priors file:'propinit.txt'
! b)Parameters:
! -Number of parameters: Npar
! -Total number of steps to take: MSim
! -Burn in  steps: Nburn
! -Length of chains: NSim
! OUTPUTS:
! Files:
! -Chains of :'mcmc_data.txt'
!-------------------------------------------------
!-------Declaration of variables------------
        implicit none
dimension oldTheta(15),oldTheta_cl(1000),proposed(15),
     $  proposed_cl(1000),Theta(100000,15),l_map(1000),lt(2000),
     $ cl_map(1000),err_map(1000),cl_thp(2000),cltheory(100000,1000),
     $  propo(15),LgLike(100000),chi2(100000),chi2_dof(100000),
     $  sig_par(15),start(15),fin(15),sig_para(15),sigma(15),
     $  z2_min(100000),propoz2(100000),
     $  a(2000),wa(2000)
real StartChain,oldTheta,oldTheta_cl,proposed,proposed_cl,da,
     $  Theta,cl_map,err_map,cl_thp,cltheory,propo,
     $ LgLike,X,Y,w0,w1,z1,z2,delta,propLike,oldLike,chi2,chi2_dof,
     $  sig_par,start,fin,sig_para,sigma,
     $  sqdiff,beta,z2_min,maxz, propoz2,a,wa
          integer Npar,mdata,iSim,MSim,ml,Nburn,mt,i,iprop,NSim,iproposed,
```

```
     $  l_map,lt,ith,ia,it,wasize
!------Opening input files-------
open(unit=1,file='wzparams.txt~',status='old') !Model input
open(unit=3,file='wmap_bin_tt_pws5.txt',
     $  status='old')!WMAP 5years tt binned data input
open(unit=4,file='propinit.txt',status='old') !Priors input
        open(unit=5,file='wa.dat',status='unknown')
! Reading from input file 1(model input)
read(1,*,end=10) Theta(1,1),Theta(1,2),Theta(1,3),Theta(1,4),
     $ Theta(1,5),Theta(1,6),Theta(1,7),Theta(1,8),Theta(1,9),
     $  Theta(1,10),Theta(1,11) ! a row vector of 5 columns
10 close(1)
!  Note !Theta(1,1)=w0,Theta(1,2)=w1,Theta(1,3)=z1,Theta(1,4)=z2,
!       Theta(1,5)=delta,Theta(1,6)=Hubble,Theta(1,7)=OmegaB,
! Theta(1,8)=OmegaDMTheta(1,9)=OmegaDE,Theta(1,10)=ns,
! Theta(1,11)=optical density.
! Reading from WMAP 5years tt binned data input
mdata=1
75 read(3,*,end=81) l_map(mdata),cl_map(mdata),err_map(mdata) !(43 lines)
mdata=mdata+1
goto 75
81 close(3)
mdata=mdata-1
!------Reading priors-------
Npar=1
```

```
89 read(4,*,end=91) sig_par(Npar),start(Npar),fin(Npar) !priors on standard
!       deviation and ranges
Npar=Npar+1
goto 89
91 close(4)
Npar=Npar-1 ! Number of parameters after this loop becomes five(Npar=5)
!-------Setting the length of Monte Carlo simulations------------
        Nburn=0 !Number of Monte Carlo Steps designated for the burn in phase
NSim=30000 !Number of Monte Carlo Steps
MSim=Nburn+NSim !and total number of steps
!--------Calling the linux commands for resetting----------------
call system('rm input')! Removing previous input parameter values
call system('cp wzparams.txt~ wzparams.txt')! Get input parameters.
call system('rm mcmc_data.txt')! Removing previous outputs.
        call system('rm cl_comp.txt')
call system('rm proposed_steps.txt')
!--------creating a wafile used in CAMB(file params.ini) for w ----
!--------parametrization-------
        wasize=100
        call wdyn_func(wasize,Theta(1,1),Theta(1,2),Theta(1,3),
     $  Theta(1,4),Theta(1,5),a,wa)
        do ia=1,wasize
         write(5,*) a(ia),wa(ia)
        enddo
        close(5)
```

```
! ----------Changing  parameters in params.ini run CAMB to obtain-----
!----------- the output (cls)
           call system('./cambtest.script')
!-----------Opening and read the theorectical cls from CAMB output--------
open(unit=17,file='cambcls.txt',status='old')
continue
        write(*,*) 'Initial cls read'
!---------Only picking theoretical cls corresponding to the multipole --------
!---------values we have in WMAP data.----------
        do it=1,1999
read(17,*) lt(it),cl_thp(it)
        enddo
do ml=1,mdata
   cltheory(1,ml)=cl_thp(ml)
enddo
close(17)
!-------------Begin Monte Carlo Loop--------------
-----------------------------------------------------
write(*,*) 'begin Monte'
do iSim=2,MSim+1
!---------Older position in the parameter space-------------
   do i=1,Npar
      oldTheta(i)=Theta(iSim-1,i)
   enddo
   do ml=1,mdata
```

```
      oldTheta_cl(ml)=cltheory(iSim-1,ml)
   enddo
101       call Proposal(propo,oldTheta,sig_par,sig_para,sigma,
     $         start,fin,Npar,proposed)
               z2_min(iSim)= 1.0 +((proposed(7)+proposed(8))/(-1.0*
     $         proposed(9))*(1/(1+3*proposed(1))))**(1/(3*proposed(2)))*
     $         (1+proposed(3))**((proposed(2)-proposed(1))/proposed(2))
               beta=0.5
               if (beta*z2_min(iSim).lt.proposed(4)) then
                  maxz=proposed(4)
      else
                  maxz=beta*z2_min(iSim)
      endif
!----------Finding the value less than 950-------
               if (maxz.lt.950) then
         proposed(4)=maxz
      else
!------------call proposal subroutine  again------
                  goto 101
      endif
!------------ Storing proposed parameter positions-------------
   open(unit=9,file='wzparams.txt',status='unknown')!scratch file
            write(9,'(f15.9," ",f15.9," ",f15.9," ",f15.9," ",f15.9," ",
     $      f15.9," ",f15.9," ",f15.9," ",f15.9," ",f15.9," ",f15.9)')
     $      proposed(1),proposed(2),proposed(3),proposed(4), proposed(5),
```

```
     $     proposed(6),proposed(7),proposed(8),proposed(9),proposed(10),
     $    proposed(11)
   close(9)
   write(*,*) 'next call'
!-------Getting theorectical cls for the new proposed parameter values----
!--------Preparing a wa file------------
           open(unit=5,file='wa.dat',status='unknown')
           call wdyn_func(wasize,proposed(1),proposed(2),proposed(3),
     $     proposed(4),proposed(5),a,wa)
           do ia=1,wasize
            write(5,*) a(ia),wa(ia)
           enddo
           close(5)
   call system('./cambtest.script')
!-----------Only picking theorectical cls corresponding to the multipole-----
!-----------values we are having  in WMAP data-------------
   open(unit=17,file='cambcls.txt',status='unknown') !scratch file
           do it=1,1999
   read(17,*) lt(it),cl_thp(it)
           enddo
   do ml=1,mdata
   proposed_cl(ml)=cl_thp(ml) !Selection
   enddo
   close(17)
!--------Evaluate proposed position-------------
```

```
      call EvaluateTheta(iprop,propLike,oldLike,l_map,cl_map,
      $     err_map,oldTheta_cl,proposed,proposed_cl,mdata)
   iproposed=iprop
   if (iproposed.eq.1) then
!--------single move function---------
      do i=1,Npar
         Theta(iSim,i)=proposed(i)
      enddo
      do ml=1,mdata
         cltheory(iSim,ml)=proposed_cl(ml) !Accept the proposed step
      enddo
      LgLike(iSim)=propLike!Store the proposed Loglikelihood
   else
      do i=1,Npar
         Theta(iSim,i)=oldTheta(i)
      enddo
      do ml=1,mdata
         cltheory(iSim,ml)=oldTheta_cl(ml)!Keep previous position
      enddo
      LgLike(iSim)=oldLike !store previous position
   endif
            chi2(iSim)=-2*LgLike(iSim)
            chi2_dof(iSim)=chi2(iSim)/mdata
!--------Record output data---------------
   open(unit=7,file="mcmc_data.txt",status='unknown',
```

```
     $     access='append')
   write(7,'(f15.9," ",f15.9," ",f15.9," ",f15.9," ",f15.9,
     $     " ",f15.9," ",f15.9," ",f15.9," ",f15.9," ",f15.9," ",f15.9,
     $     " ",f20.8," ",f20.8," ",f20.8)') Theta(iSim,1),Theta(iSim,2),
     $     Theta(iSim,3),Theta(iSim,4),Theta(iSim,5),Theta(iSim,6),
     $     Theta(iSim,7),Theta(iSim,8),Theta(iSim,9),Theta(iSim,10),
     $     Theta(iSim,11),chi2(iSim),chi2_dof(iSim),LgLike(iSim)
           close(7)
        enddo! Ending the main loop
stop
end
!---------------------------
! Used subroutines
!---------------------------
!-------This subroutine is for keeping parameters in a predifined r-----
!-------ange in prior file 'propint.txt'--------
subroutine Proposal(propo,oldTheta,sig_par,sig_para,sigma,
     $  start,fin,Npar,proposed)
implicit none
Dimension propo(15),oldTheta(15),sig_par(15),sig_para(15),
     $ sigma(15),start(15),fin(15),proposed(15)
real propo,oldTheta,sig_par,sig_para,sigma,start,fin,proposed
integer i,Npar,bound
! -------Make a Jump from previous step--------
202 call Jump(sig_par,sig_para,sigma,oldTheta,Npar,propo)
```

```
bound=1
do i=1,Npar
   if (propo(i).le.start(i).or.propo(i).ge.fin(i)) then !Making ----
 !----------sure that parameters are in prescribed ranges--------
      bound=0
   endif
   if (bound.eq.0) then ! we exit the loop as soon as one of the ------
!-----------parameters is out of bounds----------
      goto 202 !generating a different random number
   endif
enddo
if (bound.eq.1) then ! we only need to check if z1<z2 if all 5 params ----
!-----------are within the bounds---------
   if (propo(3).ge.propo(4)) then
      bound=0
   endif
endif
if (bound.eq.1) then
   do i=1,Npar
      proposed(i)=propo(i)
   enddo
else
   goto 202
endif
return
```

```
end
!---------The subroutine for secting sigmas accordong to parameter---------
!---------ranges from the file---------
!        propinit.txt
subroutine Jump(sig_par,sig_para,sigma,oldTheta,Npar,propo)
implicit none
Dimension sig_par(15),sig_para(15),sigma(15),oldTheta(15)
     $  ,propo(15)
real sig_par,sig_para,sigma,oldTheta,propo,X,Y
integer i,Npar
call sigma_par(oldTheta,Npar,sig_par,sig_para,sigma)
do i=1,Npar
   call GRNF(X,Y)
   propo(i)=oldTheta(i)+sigma(i)*X ! Making a random jump from ---
!------previous position
         enddo
  return
  end
!---------Make use of different standard deviation for z1,z2--------
subroutine sigma_par(oldTheta,Npar,sig_par,sig_para,sigma)
implicit none
dimension oldTheta(15),sig_par(15),sig_para(15),sigma(15)
real oldTheta,sig_par,sig_para,sigma
integer i,Npar
do i=1,Npar
```

```
   if (i.eq.3.or.i.eq.4) then
      sig_para(i)=sig_par(i)*(1+oldTheta(i))
   else
      sig_para(i)=sig_par(i)
   endif! The subroutine setting the standard deviation for------
 !-------different parameters---------
enddo
do i=1,Npar
   sigma(i)=sig_para(i)
enddo
return
end
!-------Evaluating the proposed position using the loglikelihood test-----
subroutine EvaluateTheta(iprop,propLike,oldLike,l_map,cl_map,
     $  err_map,oldTheta_cl,proposed,proposed_cl,mdata)
implicit none
dimension oldTheta_cl(1000),proposed_cl(1000),cl_map(1000),
     $  err_map(1000),l_map(1000),proposed(15)
real propLike, oldLike, diff,ediff,oldTheta_cl,proposed_cl,
     $  cl_map,err_map,chi2,proposed,rand
integer mdata,moo,iprop,l_map,i
call chisqd(proposed_cl,cl_map,err_map,l_map,chi2,mdata)
propLike=-chi2/2.0 !Loglikelihood for the proposed steps
call chisqd(oldTheta_cl,cl_map,err_map,l_map,chi2,mdata)
oldLike=-chi2/2.0!Loglikelihood for the old (previous) position
```

```
diff=propLike-oldLike
ediff=exp(diff) ! Computing the  probability of accepting next step
if (diff.gt.0.0) then
   moo=1
elseif (rand().lt.exp(diff)) then
   moo=1
else
   moo=0
endif
iprop=moo

!------In case of tasting the proposed loglikelihood,the old one-----
!------their difference------
!------the acceptance probability-------
!------and the integer logical number after evaluating are -----
!------printed on the screen.
open(unit=21,file="proposed_steps.txt",status='unknown',
     $  access='append')
write(21,'(f7.4," ",f7.4," ",f10.4," ",f10.4," ",f7.4," ",
     $  f7.4," ",f7.4," ",f7.4," ",f7.4," ",f7.4," ",f7.4," ",
     $  e20.5," ",e20.5," ",e20.5," ",e20.5," ",i2.1)')
     $  proposed(1),proposed(2),proposed(3),proposed(4),proposed(5),
     $  proposed(6),proposed(7),proposed(8),proposed(9),proposed(10),
     $  proposed(11),propLike,oldLike,diff,ediff,iprop
close(21)
```

```
        write(*,'(e20.5," ",e20.5," ",e20.5," ",e20.5," ",i2.1)')
     $  propLike,oldLike,diff,ediff,iprop
return
end
!--------Finding the chi-squared (chi2) using CAMB output and WMAP
!5year binned TT power spectrum--------
        subroutine chisqd(p_cl,cl_map,err_map,l_map,chi2,mdata)
implicit none
dimension p_cl(1000),p_diff(1000),cl_map(1000),err_map(1000),
     $  l_map(1000)
real chi2,p_cl,p_diff,cl_map,err_map
integer mdata,ith,l_map
chi2=0.
do ith=1,mdata
   p_diff(ith)=((((p_cl(ith)))
     $     -((cl_map(ith))))**2)/((err_map(ith))**2)
   chi2=chi2+p_diff(ith)
   open (unit=28,file='cl_comp.txt',status='unknown',
     $     access='append')
   write(28,'(i10.3," ",e20.8," ",e20.8," ",e20.8," ",e20.8)')
     $     l_map(ith),cl_map(ith),err_map(ith),
     $     (p_cl(ith))*(cl_map(5))/(p_cl(5)),p_diff(ith)!Comparing both ----
!---------theorectical CAMB and WMAP data cls-------
   close(28)
enddo
```

```
        write(*,'(f15.3)') chi2
return
end
!--------Random number generator subroutine---------
        SUBROUTINE GRNF(X,Y)
implicit none
REAL PI,R1,R2,X,Y,rand
   PI = 4.0*ATAN(1.0)
   R1 = -ALOG(1.0-rand())
   R2 = 2.0*PI*rand()
   R1 = SQRT(2.0*R1)
   X  = R1*COS(R2)
   Y  = R1*SIN(R2)
RETURN
END
!----------Equation of state function------------
        subroutine wdyn_func(nwa,w0,w1,z1,z2,delta,a,wa)
        implicit none
        dimension a(100),wa(100),f1(100),f2(100)
!---------equation of state for dark energy-------
        real a,a1,a2,wa,da
        real delta,w0,w1,z1,z2,f1,f2
        integer ia,nwa
a1 = 1.0/(1.0+z1)
        a2 = 1.0/(1.0+z2)
```

```
 a(1)=10e-3
 da=0.01
 do ia=1,nwa
  a(ia+1)=a(ia)+da
  f1(ia) = (tanh(((1.0/a(ia))-(1.0/a1))/delta))
  f2(ia) = (tanh(((1.0/a(ia))-(1.0/a2))/delta))
  wa(ia) = w0 + 0.5*(w1-w0)*(f1(ia) - f2(ia))
 enddo
return
end
```

B.3 Code for selecting models

```
%-------------------------------------------
%b) The code for selection of models with
%low chi-squared
%-------------------------------------------
% Matlab code to pick models with chi-squared
% per degree of freedom(p.d.o.f) in the range [1,1.9].

%DESCRIPTION:
% This code load the file containing the chain
% and then select the best fit parameters by
```

```
%taking the small value of chi-squared.
%
function testaccel_last
clear all% resetting
% Loading the file containing a chain
fo=load('mcmc_data.txt');
ch=13;% The column corresponding to the chi-squared
%p.d.f
co=find(fo(:,ch)>1.0 & fo(:,ch)<1.9);
%
fch=fo(co,:);
indo=unique(fch(:,ch));% Avoiding repeatition
chi=fo(indo,:);
[m,n]=size(chi);% Getting the size of unprepeated
%steps for chi-squares p.d.o.f
save('chifit21.txt', 'chi*', '-ASCII')%Saving that
%to a file.
% Setting random indexes for selecting randomly
%some of the tolal steps.
ri=randi(m,[20,1]);
zt=0:0.05:1000; %redshift interval and range
nzt=length(zt);
%[m n]=size(par);
% pause
% paraameters
```

```
G=6.67e-11;
for i=ri
 for  j=1:nzt
  %W(z) parameters
  w0(i)=fo(i,1);
  w1(i)=fo(i,2);
  z1(i)=fo(i,3);%first redshift
  z2(i)=fo(i,4);%second redshift
  delta(i)=fo(i,5);%transition width
  %Other parameters involved in the
  %calculation of acceleration
   H0(i)=fo(i,6);% Hubble parameter
   Omega0(i)=fo(i,9);% gark energy
   Omegam0(i)=fo(i,8)+fo(i,7);%cold matter
  % Writing our parametrization
   f1(i,j) = (tanh(((1+zt(j))-(1+z1(i)))./delta(i)));
   f2(i,j) = (tanh(((1+zt(j))-(1+z2(i)))./delta(i)));
   wz(i,j) = w0(i) + 0.5.*(w1(i)-w0(i)).*(f1(i,j) - f2(i,j));

  % We want to evaluate
  %rhode(z)=rhode0.exp(3.*integral(1+w(z))./(1+z),0,z)))
   fz1(i,j)=(1+w0(i)).*log(1+zt(j));
   y(i,j)= 0.5.*(w1(i)-w0(i)).*(tanh((zt(j)-z1(i))./delta(i))-...
        tanh((zt(j)-z2(i))/delta(i))).*(1+zt(j));
```

```
  end
end
   %Integrating using cumsimpson a function
   % provided in Mathworks.
   fz2=cumsimpson(zt',y');
   %rhod=rhode0.*exp(3.*(fz1+fz2'));
   fz=exp(3.*(fz1+fz2'));
   %Looping over models to get acceleration
for k=1:m
  for l=1:nzt
       Q(k,l)=-(Omegam0(k).*(1+zt(l)).^(3)+Omega0(k)*...
           fz(k,l).*(1+3.*wz(k,l)));%acceleration using the
   %the acceleration equation
    end
end


  figure(1)
  plot(zt,Q(ri,:))% ploting acceleration for selected models.
  axes('position',[0.175 0.25 0.175 0.25]) %choosing the size for the subplot
  plot(zt,Q(ri,:))
  axis([0 2 -0.69 1])
```

B.4 Code for plotting the CMB power spectrum and w(z)

```
%THIS CODE PLOTS EQUATION OF STATE FOR A DOUBLE KINK
%PARAMETRIZATION AND THE CMB POWERSPECTRUM CORRESPONDING
%TO THE CHOSEN PARAMETER
%%%%%%%%%%%%%%%%%%%%%%%%%%%%
params = load('params.txt');% loading the file parameters.
cl = load('p_spect.dat');% loading the multiple moment and
%cmb power spectrum from camb
l = cl(:,1);
map = colormap('lines');
z = 0:0.01:100; %The redshift used in finding the values of
%equation of state w(z)
a = 1./(1+z);% The scalar factors
wvec = 1:size(params,1); %Rows in the used parameters file
for i = wvec
    wo = params(i,1); %First parameter
    w1 = params(i,2); %Second parameter
    z1 = params(i,3); %Third parameter
    z2 = params(i,4); %fourth parameter
    dela = params(i,5);%fith parameter
    a1 = 1./(1+z1);
    a2 = 1./(1+z2);
% DOUBLE KINK PARAMETRIZATION
```

```
    f1 = (tanh(((1.0d0./a)-(1.0d0./a1))./dela));
    f2 = (tanh(((1.0d0./a)-(1.0d0./a2))./dela));
    wz= wo + 0.5*(w1-wo)*(f1 - f2);
    figure(1)
    plot(z,wz,'color',map(i,:)), hold on % plotting the equation of state
% CMB POWERSPECTRUM FORM CAMB
    figure(2)
    semilogx(l,cl(i,l)./max(cl(i,l)),'color',map(i,:)), hold on % Plotting
%the power sppectum
end
% WMAP FIVE YEAR TT POWER SPECTRUM PLOTTING;
    cl_wmap5 = load('wmap_binned_tt_spectrum_5yr_v3.txt'); %loading
%the WMAP5 data
    errorbar(cl_wmap5(:,1),cl_wmap5(:,4)./max(cl_wmap5(:,4)),...
    cl_wmap5(:,5)./max(cl_wmap5(:,4)),'.'), hold on % Plotting
%WMAP5 data with errorbars.
```

B.5 Dark energy and dark matter density using the double kink parameterization

```
 %THIS CODE IS FOR FINDING THE DENSITY PARAMETER VALUES
%FOR CONSIDERED MODELS
function Omegad
clear all
```

```
p=load('para.txt'); %Loading the parameter file
zt=0.001:0.01:7;% redshift range
nzt=length(zt);% the length of the redshift vector
[m n]=size(p); % size of the data file
map=colormap('lines'); % color map
%Start looping over models with parameters: w0, w1, z1, z2, delta.
for i=1:m
  for  j=1:nzt
w0(i)=p(i,1);
w1(i)=p(i,2);
z1(i)=p(i,3);
z2(i)=p(i,4);
delta(i)=p(i,5);
%CONSTANTS
H0=70; %Hubble parameter
G=6.67e-11; %Gravitational constant
Omega0=0.7; %Dark energy density parameter
Omegam0=0.3;% Dark matter density parameter
rhode0=Omega0.*3.*H0.^2./(8.*pi.*G); %Dark energy density today.
%loop=1;

% We want to evaluate the rhode(z)=rhode0.*3.*integral(1+w(z)).
%/(1+z),0,z)(equation 3.3)
f1(i,j)=(1+w0(i)).*log(1+zt(j));
F=@(x)(tanh((x-z1)./delta)-tanh((x-z2)./delta))./(1+x);%The integrand
```

```
f2(i,j)=(w1(i)-w0(i)).*quadl(F,0,zt(j)); % Integrating using
% 'quadl' function
rhod(i,j)=rhode0.*exp(3.*(f1(i,j)+f2(i,j))); % Getting
%dark density
% Plotting the dark energy density
plot(zt(j),rhod(i,j),'color',map(i,:)), hold on
end
```

References

ABAZAJIAN, K. *et al.* (2004). The Second Data Release of the Sloan Digital Sky Survey. *Astron. J.*, **128**, 502–512. 1

AFSHORDI, N., LOH, Y.S. & STRAUSS, M.A. (2004). Cross-Correlation of the Cosmic Microwave Background with the 2MASS Galaxy Survey: Signatures of Dark Energy, Hot Gas, and Point Sources. *Phys. Rev.*, **D69**, 083524. 17

AMSLER, C. *et al.* (2008). Review of particle physics. *Phys. Lett.*, **B667**, 246–253. 21

ANDRIEU, C., DEFREITAS, N., DOUCET, A. & JORDAN, M.I. (2003). An Introduction to MCMC for Machine Learning. *Machine Learning*, **50**, 5–43. 45

ARMENDARIZ-PICON, C., MUKHANOV, V.F. & STEINHARDT, P.J. (2000). A dynamical Solution to the Problem of a Small Cosmological Constant and Late-time Cosmic Acceleration. *Phys. Rev. Lett.*, **85**, 4438–4441. 27

ASTIER, P. *et al.* (2006). The Supernova Legacy Survey: Measurement of Omega(M), Omega(Lambda) and w from the First Year Data Set. *Astron. Astrophys.*, **447**, 31–48. 21

BASHINSKY, S. & BERTSCHINGER, E. (2002). Dynamics of cosmological perturbations in position space. *Phys. Rev.*, **D65**, 123008. 50

BASSETT, B.A., KUNZ, M., SILK, J. & UNGARELLI, C. (2002). A late-time transition in the cosmic dark energy? *Mon. Not. Roy. Astron. Soc.*, **336**, 1217–1222. 3, 30, 32, 49

BASSETT, B.A., CORASANITI, P.S. & KUNZ, M. (2004). The Essence of Quintessence and the Cost of Compression. *Astrophys. J.*, **617**, L1–L4. 30, 49

BERNARDEAU, F., COLOMBI, S., GAZTANAGA, E. & SCOCCIMARRO, R. (2002). Large-scale structure of the Universe and Cosmological perturbation theory. *Phys. Rept.*, **367**, 1–248. 14

BOUGHN, S. & CRITTENDEN, R. (2004). A correlation of the cosmic microwave sky with large scale structure. *Nature*, **427**, 45–47. 18

BURIGANA, C. (2007). Sunyaev-Zeldovich and Cosmic Microwave Background. *PoS*, **MCCT-SKADS**, 013. 24

CAHN, R.N., DE PUTTER, R. & LINDER, E.V. (2008). Field Flows of Dark Energy. *JCAP*, **0811**, 015. 25

CALDWELL, R.R. (2002). A Phantom Menace? *Phys. Lett.*, **B545**, 23–29. 28

CALDWELL, R.R. & DORAN, M. (2004). Cosmic Microwave Background and Supernova Constraints on Quintessence: Concordance Regions and Target Models. *Phys. Rev.*, **D69**, 103517. vi, 28, 29

CALDWELL, R.R., DAVE, R. & STEINHARDT, P.J. (1998). Cosmological imprint of an energy component with general equation of state. *Phys. Rev. Lett.*, **80**, 1582–1585. 3, 25, 26

CALDWELL, R.R., KAMIONKOWSKI, M. & WEINBERG, N.N. (2003). Phantom energy. *Phys. Rev. Lett.*, **91**, 071301. 3, 25

CARROLL, S.M. (2001). The cosmological constant. *Living Rev. Rel.*, **4**, 1. vi, 2, 23

CHAKRABORTY, W. & DEBNATH, U. (2007). Is modified Chaplygin gas along with barotropic fluid responsible for acceleration of the universe? *Mod. Phys. Lett.*, **A22**, 1805–1812. 3

CHIMENTO, L.P., FORTE, M., KREMER, G.M. & RICHARTE, M.G. (2009). Tachyon and Quintessence Brane-World Universe. *Phys. Rev.*, **A79**, 083527. 25

COPELAND, E.J., SAMI, M. & TSUJIKAWA, S. (2006). Dynamics of dark energy. *Int. J. Mod. Phys.*, **D15**, 1753–1936. 27, 30

CORASANITI, P.S., KUNZ, M., PARKINSON, D., COPELAND, E.J. & BASSETT, B.A. (2004). The Foundations of Observing Dark Energy Dynamics with the Wilkinson Microwave Anisotropy Probe. *Phys. Rev.*, **D70**, 083006. vi, 28, 30, 31

CORASANITI, P.S., GIANNANTONIO, T. & MELCHIORRI, A. (2005). Constraining dark energy with cross-correlated CMB and Large Scale Structure data. *Phys. Rev.*, **D71**, 123521. vi, 20

DEBNATH, U. (2007). Variable Modified Chaplygin Gas and Accelerating Universe. *Astrophys. Space Sci.*, **312**, 295–299. 3

DES-PROJECT (2009). Dark Energy Survey project site. `https://www.darkenergysurvey.org/the-project`, [Online; accessed 30-July-2009]. 24

DUNKLEY, J. *et al.* (2009). Five-Year Wilkinson Microwave Anisotropy Probe (WMAP) Observations: Likelihoods and Parameters from the WMAP data. *Astrophys. J. Suppl.*, **180**, 306–329. vii, 43, 44

EISENSTEIN, D.J. & HU, W. (1997). Power Spectra for Cold Dark Matter and its Variants. *Astrophys. J.*, **511**, 5. 16

FOSALBA, P. & GAZTANAGA, E. (2004). Measurement of the Gravitational Potential Evolution from the Cross-correlation between WMAP and the APM Galaxy survey. *Mon. Not. Roy. Astron. Soc.*, **350**, L37–L41. 18

FRENK, C.S., WHITE, S.D.M., BODE, P., BOND, R.J., BRYAN, G.L., CEN, R., COUCHMAN, H.M.P., EVRARD, A.E., GNEDIN, N., JENKINS, A., KHOKHLOV, A.M., KLYPIN, A. & AND, J.F.N. (1999). The santa barbara cluster comparison project: a test of cosmological hydrodynamics codes. `http://citeseer.ist.psu.edu/118324.html`. 24

FRIEMAN, J., TURNER, M. & HUTERER, D. (2008). Dark Energy and the Accelerating Universe. *Ann. Rev. Astron. Astrophys.*, **46**, 385–432. vi, 9, 13, 15, 21, 22, 24, 26, 28

FRIEMAN, J.A. (2008). Lectures on dark energy and cosmic acceleration. *AIP Conf. Proc.*, **1057**, 87–124. 21

GAZTANAGA, E., MANERA, M. & MULTAMAKI, T. (2006). New light on dark cosmos. *Mon. Not. Roy. Astron. Soc.*, **365**, 171–177. 17, 18

GELMAN, A., ROBERTS, G.O. & GILKS, W.R. (1996). *Efficient Metropolis jumping rules. Bayesian statistics*. Oxford Univ. Press. 47

GOLDHABER, G. *et al.* (2001). Timescale Stretch Parameterization of Type Ia Supernova B- band Light Curves. *Astrophys. J.*, **558**, 359–368. 21

GUNN, J.E. & TINSLEY, B. (1976). Dynamical friction - the hubble diagram as a cosmological test. *ApJ*, **210**, 457–457. 1

HARRISON, E. (1993). The redshift-distance and velocity-distance laws. *ApJ*, **403**, 28–31. 10

HASTINGS, W.K. (1970). Monte carlo sampling methods using markov chains and their applications. *Biometrika*, **57**, 97–109. 46

HOYLE, F. & NARLIKAR, J.V. (1964). On the Avoidance of Singularities in C-Field Cosmology. *Royal Society of London Proceedings Series A*, **278**, 465–478. 28

HU, W. & DODELSON, S. (2002). Cosmic Microwave Background Anisotropies. *Ann. Rev. Astron. Astrophys.*, **40**, 171–216. 17

HUBBLE, E. (1929). A Relation between Distance and Radial Velocity among Extra-Galactic Nebulae. *Proceedings of the National Academy of Science*, **15**, 168–173. 6

HUTERER, D. & STARKMAN, G. (2003). Parameterization of dark-energy properties: A principal- component approach. *Phys. Rev. Lett.*, **90**, 031301. 3

IVEZIC, Z. *et al.* (2008). LSST: from Science Drivers to Reference Design and Anticipated Data Products. `astro-ph/0805.2366`. 24

JAFFE, A.H. *et al.* (2001). Cosmology from Maxima-1, Boomerang and COBE/DMR CMB Observations. *Phys. Rev. Lett.*, **86**, 3475–3479. 8

KOLDA, C.F. & LYTH, D.H. (1999). Quintessential difficulties. *Phys. Lett.*, **B458**, 197–201. 3, 25, 27

KOMATSU, E. *et al.* (2009). Five-Year Wilkinson Microwave Anisotropy Probe (WMAP/altaffilmark 1) Observations:Cosmological Interpretation. *Astrophys. J. Suppl.*, **180**, 330–376. 8

LAZKOZ, R. (2007). Geometrical constraints on dark energy models. *AIP Conf. Proc.*, **960**, 3–32. 3, 25

LEWIS, A., CHALLINOR, A. & LASENBY, A. (2000). Efficient Computation of CMB anisotropies in closed FRW models. *Astrophys. J.*, **538**, 473–476. vi, 19, 35, 48

LINDER, E.V. (2004). Strong gravitational lensing and dark energy complementarity. *Phys. Rev.*, **D70**, 043534. 1

MARCOS, B., BAERTSCHIGER, T., JOYCE, M., GABRIELLI, A. & SYLOS LABINI, F. (2006). Linear perturbative theory of the discrete cosmological N- body problem. *Phys. Rev.*, **D73**, 103507. 14

MENGERSEN, K.L. & TWEEDIE, R.L. (1996). Rates of convergence of the hastings and metropolis algorithms. *Ann. Statist.*, **24**. 47

METROPOLIS, N., ARIANNA, W.R., MARSHALL, N.R. & AUGUSTA, H.T. (1953). Equation of State Calculations by Fast Computing Machines. *The Journal of Chemical Physics*, **21**, 1087–1092. 46

MIKNAITIS, G. *et al.* (2007). The ESSENCE Supernova Survey: Survey Optimization, Observations, and Supernova Photometry. *Astrophys. J.*, **666**, 674. 21

NASA (2008a). Derived cosmic microwave background (cmb) products. `http://lambda.gsfc.nasa.gov/product/map/current/m_products.cfm`, [Online; accessed 02-August-2008]. 35

NASA (2008b). What is the Universe made of? `http://map.gsfc.nasa.gov/universe/uni_matter.html`, [Online; accessed 30-June-2009]. 9

NASA (2008c). WMAP Cosmological Parameters. `http://lambda.gsfc.nasa.gov/product/map/dr3/params/lcdm_sz_lens_wmap5.cfm`, [Online; accessed 02-August-2008]. 43

NASA/WMAP/SCIENCE/TEAM (2009). Universe contents. `http://map.gsfc.nasa.gov/media/080998/index.html`, [Online; accessed 24-May-2009]. vi, 9

NESSERIS, S. & PERIVOLAROPOULOS, L. (2004). The fate of bound systems in phantom and quintessence cosmologies. *Phys. Rev.*, **D70**, 123529. 28

PEEBLES, P.J.E. (1980). *Research supported by the National Science Foundation. Princeton, N.J., Princeton University Press, 1980. 435 p.*. Peebles, P. J. E., provided by the SAO/NASA Astrophysics Data System. 15

PERLMUTTER, S., TURNER, M.S. & WHITE, M.J. (1999a). Constraining dark energy with SNe Ia and large-scale structure. *Phys. Rev. Lett.*, **83**, 670–673. 1, 21

PERLMUTTER, S. *et al.* (1999b). Measurements of Omega and Lambda from 42 High-Redshift Supernovae. *Astrophys. J.*, **517**, 565–586. 22

REFREGIER, A. *et al.* (2006). DUNE: The Dark Universe Explorer. `astro-ph/0610062`. 24

RIESS, A.G. *et al.* (1998). Observational Evidence from Supernovae for an Accelerating Universe and a Cosmological Constant. *Astron. J.*, **116**, 1009–1038. 1, 21

RIESS, A.G. *et al.* (2000). Tests of the Accelerating Universe with Near-Infrared Observations of a High-Redshift Type Ia Supernova. *Astrophys. J.*, **536**, 62. 22

ROBERTS, G.O. & TWEEDIE, R.L. (1996). Exponential convergence of langevin distributions and their discrete approximations. *Bernoulli*, **2**, 341–363. 47

SACHS, R.K. & WOLFE, A.M. (1967). Perturbations of a cosmological model and angular variations of the microwave background. *Astrophys. J.*, **147**, 73–90. 17

SAHNI, V. & STAROBINSKY, A. (2006). Reconstructing Dark Energy. *Int. J. Mod. Phys.*, **D15**, 2105–2132. 3

SAHNI, V. & STAROBINSKY, A.A. (2000). The Case for a Positive Cosmological Lambda-term. *Int. J. Mod. Phys.*, **D9**, 373–444. 25, 26, 27, 28

SAPONE, D., KUNZ, M. & KUNZ, M. (2009). Fingerprinting Dark Energy. *Phys. Rev.*, **D80**, 083519. 17

SCRANTON, R. *et al.* (2003). Physical Evidence for Dark Energy. *Phys. Rev. Letters*. 18

SHAPIRO, I.L. (2008). Effective Action of Vacuum: Semiclassical Approach. *Class. Quant. Grav.*, **25**, 103001. 2

SILVESTRI, A. & TRODDEN, M. (2009). Approaches to Understanding Cosmic Acceleration. *Rept. Prog. Phys.*, **72**, 096901. 6

SIMONSEN, J.T. & HANNESTAD, S. (1999). Can Dust Segregation Mimic a Cosmological Constant? *Astron. Astrophys.*, **351**, 1–9. 22

SMOOT, G.F. *et al.* (1992). Structure in the COBE differential microwave radiometer first year maps. *Astrophys. J.*, **396**, L1–L5. 17

SOTIRIOU, T.P. & FARAONI, V. (2008). f(R) Theories Of Gravity. `gr-qc/0805.1726`. 3, 25

SPALL, JAMES C. (2003). *Introduction to Stochastic Search and Optimization.* Wiley-Interscience. 46

SPERGEL, D.N. *et al.* (2003). First Year Wilkinson Microwave Anisotropy Probe (WMAP) Observations: Determination of Cosmological Parameters. *Astrophys. J. Suppl.*, **148**, 175–194. 1, 5

SULENTIC, J.W., ZAMFIR, S., MARZIANI, P. & DULTZIN, D. (2007). Our Search for an H-R Diagram of Quasars. 1

WANG, Y. & LOVELACE, G. (2001). Unbiased estimate of dark energy density from type IA supernova data. *Astrophys. J.*, **562**, L115–L120. 3

WANG, Y., KRATOCHVIL, J.M., LINDE, A. & SHMAKOVA, M. (2004). Current Observational Constraints on Cosmic Doomsday. *JCAP*, **0412**, 006. 3, 25

ZALDARRIAGA, M. & SELJAK, U. (2000). CMBFAST for spatially closed universes. *Astrophys. J. Suppl.*, **129**, 431–434. 48

ZOLTAN HAIMAN AND JOSEPH J. MOHR AND GILBERT P. HOLDER (2001). Clusters in the precision cosmology era. *RELATIVISTIC ASTROPHYSICS: 20th Texas Symposium*, **586**, 303–309. 24